TRANSPORT STUDIES IN HAWKINS AND TOWN FARM BAYS LAKE CHAMPLAIN, VERMONT

Final Report

prepared for

Department of Buildings
State of Vermont
Montpelier, Vermont

by

Jeffrey P. Laible, Ph.D., P.E.

and

William W. Walker, Jr., Ph.D.

January 1987

TRANSPORT STUDIES IN HAWKINS AND TOWN FARM BAYS LAKE CHAMPLAIN, VERMONT

Final Report

prepared for

Department of Buildings
State of Vermont
Montpelier, Vermont

by

Jeffrey P. Laible, Ph.D., P.E.

and

William W. Walker, Jr., Ph.D.

January 1987

TABLE OF CONTENTS

INTRODUCTION

Field studies were conducted in the Hawkins Bay area during August and September of 1986. These studies were designed to obtain data for use in testing and refining the hydrodynamic and transport models previously developed for predicting the effects of an offshore discharge from the proposed Kingsland Bay Fish Hatchery on phosphorus concentrations in the area (Walker, Laible, Owens, & Effler, 1986). Additional objectives were to select a specific location for the offshore discharge and to evaluate currents in that area via drogue and dye studies. Based upon these additional data and further analysis of historical data, the phosphorus transport model has been refined and used to project hatchery impacts for effluent flows and concentrations specified in the discharge permit which has been drafted by the Vermont Department of Water Resources. The work is described in the following sections:

WIND VELOCITY MEASUREMENTS
DROGUE STUDIES
DISCUSSION OF CURRENT PATTERNS AT PROPOSED OUTFALL LOCATION
DYE STUDIES
TRANSPORT MODEL REFINEMENTS
HATCHERY IMPACT PROJECTIONS

A final section summarizes principal conclusions of the study. The location of the proposed offshore outfall is approximately 400 meters west of Gardiner Island, as shown in Figure 1. Results indicate that, with the proposed effluent limitations, the offshore hatchery discharge will cause an average increase of less than 2 ppb in the bay area east and south of Thompson's Point under summer loading and wind conditions.

WIND VELOCITY MEASUREMENTS

Wind speed and direction were recorded at the eastern tip of Thompson's Point during August and September 1986, as shown in Figure 1.

Measurements were recorded at 5-minute intervals using a remote data logger. Wind speeds driving lake currents are likely under-estimated because the field station is somewhat sheltered by land masses, particularly from northeast winds.

The resulting wind rose is shown in Figure 2. The data suggest two dominant wind events - southeast (mean speed = 7.3 mph) and northwest (mean speed = 6.6 mph). The mean wind speed for August-September 1986 period was 8.7 mph, compared with a 20-year average of 7.7 mph recorded at the Burlington Airport for these months. Figures 3-6 display the wind speed and direction for time periods preceding and during each drogue study.

Wind speed and direction at Thompson's Point during September 1986 are compared with the Burlington Airport data in Figures 7 and 8, respectively. The lake data are more scattered because the observations are at 5-minute intervals, as compared with the Burlington Airport data, which are taken at 3 hr intervals. With the exception of the northern wind event which occurred on September 20, speed and direction are in reasonable agreement. Burlington Airport data appear useful for longterm projections, although both sources of wind data seem likely to underestimate wind speeds over the lake.

Histograms of wind direction at Thompson's Point and Burlington Airport wind data are shown in Figures 9 and 10. Wind is from the SE quadrant 44,45% of the time at the Airport and the lake site respectively. The percentages for the other quadrants for the airport and lake site respectively are NE - 13,20 %, SW - 12,10% and NW-30,26%. When broken down into eight directions (Figure 10), the data indicate that winds are more from the SE at the lake site than at the Airport.

DROGUE STUDIES

During the August-September 1986 period of field studies, lake elevations averaged 96.3 feet, or .7 feet above the mean stage of 95.6 feet. Drogues, devices used for direct measurement of lake current velocities, were released and tracked on four occasions. Wind conditions, release points, and drogue paths are summarized in Figure 11. Drogue paths are compared with model predictions as follows:

Release	Paths	Hodographs*
August 18	Figure 12	Figure 13
August 28	Figure 14	Figure 15
Sept 2	Figure 16	Figure 17
Sept 3	Figure 17	Figure 19

* velocity vs. depth diagrams

Table 1 summarizes measured and modeled current speeds. Results indicate that there is a dominant current along a NE-SW bearing for both NW and SE wind conditions and that the hydrodynamic model generally underpredicts measured current speeds, when driven by wind speeds measured at Thompson's Point.

On August 18, the mean wind velocity prior to and during drogue tracking has been computed using wind data from 9:30 - 15:00. The mean velocity was 13.8 mph from a direction 25 degrees west of true north. Figure 12 shows the August 18 wind direction (NNW), predicted vertically averaged current patterns, and the observed drogue paths. The modeled currents have been generated using a wind speed of 13.8 mph and a wind shear coefficient C_w=.001 (identical to the value used in previous simulations (Walker et al., 1986)). The model hodograph at node (82) nearest to the release point, is shown in Figure 13, along with the observed drogue paths.

Initial drogue path directions compare well with the simulated patterns for the August 18 drogue study. The drogue paths follow the directions of the simulated currents away from the release point. Both the modeled and measured results suggest a strong reverse current, with a mean direction towards the northwest. Measured current magnitudes were approximately twice the modeled currents near the surface. The observed and predicted magnitudes at the lower depths were in good agreement, however.

On August 28, wind direction was initially from the NW (prior to 11 am), but later shifted to the NE. Wind speeds varied from 5-13 mph. Figure 14 shows the simulated current patterns for a N wind and the drogue paths. Figure 15 compares the drogue paths and the simulated flow over the depth. Observed currents (3.9-8.5 cm/sec) are significantly larger then the simulated values (1.6-4.2 cm/sec). Simulated surface currents are in the direction of the wind, whereas the observed currents were directly into the wind. Both observed and simulated flows are generally along a NE-SW bearing.

On September 2, the wind was from the W-NW direction at 5-10 mph. Figure 16 shows the simulated current patterns for WNW wind and the drogue paths. Figure 17 compares the drogues paths and simulated flow over the depth. In this case, the directions of the surface and bottom currents are in good agreement. The observed flows from 1 meter down are again along a NE-SW bearing. This case gives the best agreement with the magnitude of flow. Observed and simulated surface speeds are 2-3 cm/sec vs. 2 cm/sec, respectively. Observed and simulated near-bottom speeds are 2-3 cm/sec vs. 1 cm/sec, respectively.

On September 3, the mean wind velocity prior to and during tracking was computed using wind data from 8:00 - 16:00. The mean velocity was 9.3 mph from a direction 25 degrees east of true south. Figure 18 shows the September 3 wind direction (SSE), predicted vertically averaged current patterns, and observed drogue paths. The model hodograph at

node 92, nearest to the September 3 release point, is shown in Figure 19, along with the observed drogue paths.

The initial drogue path directions compare well with simulated patterns for the September 3 release. The drogue paths also follow the directions of the simulated currents away from the release point. Both the modeled and measured current structures are predominantly towards the northeast. The model predicts a mild reverse current which was not observed in the field. Observed current magnitudes on this date are significantly greater (4 - 8 times) than the modeled currents. This indicates that the assumed wind shear coefficient may be too low and/or that a slope current had not fully developed (see discussion below).

One possible explanation for the better agreement of the modeled and measured currents for the NNW case is that the magnitude and direction of the wind on August 18 was steadier and of longer duration than on September 3 (SSE event). Since the model produces results for a steady condition, better agreement should be achieved for winds of a stronger and longer duration. A reverse current, as observed for the NNW event, requires a build-up in surface elevation at the windward land mass. This would be achieved more rapidly for strong winds from the NNW due to shallow area of Hawkins Bay. A longer period of time may be required for a SSE event because of the large expanse of water to the NW of the release point. These considerations suggest that the drogue paths observed on September 3 (SSE event) may have represented transient conditions, with insufficient time for full development of a reverse current. Consequently, the field measurements show more of a unidirectional flow condition.

For each drogue study, dominant observed and measured currents in the discharge region tend to be in a direction nearly perpendicular to the wind, reflecting the topographic gyre that develops throughout Hawkins and Town Farm Bays. The gyre is counter-clockwise for a SSE wind and clockwise for a NNW wind.

DISCUSSION OF CURRENT PATTERNS AT PROPOSED OUTFALL LOCATION

The previous study (Walker,Laible, Owens, & Effler, 1986) utilized wind-driven circulations as the advective terms in the cell model transport analysis. The drogue studies and modeling discussed above indicate that the hydrodynamic model captures the general structure of the circulation patterns in the region, but generally under-predicts current magnitudes.

The nature of these currents and their effects on transport in the discharge location deserve comment. Figure 20 shows simulated current patterns for eight wind conditions (N,NE,E,SE,S,SW,W and NW). While the dominant wind conditions are from the SE and NW, an interesting condition exists in the discharge cell that is common to all wind conditions. Careful observation of the direction of flow in the discharge region reveals that the discharged fluid is generally swept into currents with a NE-SW bearing. The worst condition appears to be during an easterly wind event, when the initial NE transport is drawn into Hawkins Bay near Long Point. Currents are directed into Hawkins Bay in the discharge zone during an easterly event since fluid must be replaced by the significant westerly flow along MacDonough Point. It should be noted, however, that easterly winds are present only 16% of the time (Figure 10).

These results indicate that dominant transport from the proposed discharge location is not directly into the shallow Hawkins Bay area. The results also suggest that, although the wind driven currents will tend to spread the discharged fluid throughout the greater bay area east and south of Thompson's Point, the actual direction of the wind will have little effect on changes in phosphorus concentration resulting from the hatchery discharge. The relationship between wind direction and hatchery impact is investigated further below using the transport model (see **HATCHERY IMPACT PROJECTIONS**). The proposed discharge location is favorable since it is not in a region where a particular wind condition would cause a major increase in the transport of phosphorus into the

Bay. In comparison, a discharge location closer to MacDonough Point would cause considerable transport into the Bay under S, SW, W or NW wind conditions. Flows would reverse for the N, NE, E and SE winds, respectively.

DYE STUDY

Rhodamine B dye was released at a location approximately 400 meters WNW of Gardiner Island (latitude 44° 15.04′, longitude 73° 17.71′) at 2:20 pm on September 15, 1986. The dye was released in a 150-foot strip and dispersed over a depth range of 5-25 feet. The water column was 32 feet at this location and was essentially isothermal. The quantity of dye released was sufficient to increase the average fluorescence in the release cell (column 17, row 11 of the expanded model grid) by 2.5 units, as compared with background levels of approximately .1 units.

Dye concentrations were tracked in the surrounding bays over a period of approximately two days using a flow-through fluorometer. A total of 250 measurements were recorded at depths ranging from 0 to 25 feet. Latitude/longitude coordinates were measured with a Loran-C unit. Aerial photographs of the dye plume were also taken at various times between 1 and 5 hours after the dye release to supplement the field measurements.

Wind velocity measurements at Thompson's point over the dye-study period are displayed in Figure 21. A light (2-6 mph) SE wind was dominant during the period prior to and immediately following (2 hrs) the dye release. Subsequently, dominant winds shifted between NW and NE at speeds varying up to 18 mph.

Dye measurements grouped into four time periods (2-5 hours, 5-10 hours, 21-25 hours, and 44-46 hours after the dye release) are displayed in Figure 22. The contour diagrams have been generated using the following procedure: (1) increase grid resolution by factor of 4 (divide each cell into 16 mini-cells, each 100-meters square); (2) determine

maximum observed concentration for each mini-cell and time period; (3) plot contours accordingly. Maximum (vs. mean) observed concentrations have been used to circumvent a complex spatial weighting procedure. Accordingly, the resulting contour diagrams likely over-estimate the actual dye plume concentrations and under-estimate the observed dilution.

Dye measurements, direct field observations, and aerial photographs indicate that the dye plume moved rapidly towards the ENE during the first five hours of the study. During these hours, the bulk of the measured dye mass was at depths ranging from 6 to 15 feet. Aerial photographs also indicate that a narrow surface plume extended from an area approximately 200 meters north of Gardiner Island to 400 meters west of the tip of Long Point approximately 2.5 hours after the dye release. The surface plume headed ENE to an area just north of Gardiner Island and subsequently turned NNW as it encountered currents along Long Point. This narrow surface plume was not measured directly and is not reflected in the contours shown in Figure 22. Based upon the aerial photos, the surface current velocity was approximately 8 cm/sec to the NE during the first 2.5 hours of the experiment, when light SE winds were dominant.

The behavior of the plume during the first few hours of the experiment is important because wind conditions were most representative of the prevailing SE wind. Had these winds persisted for a longer period, the bulk of the dye would likely have been transported in the counter-clockwise currents towards Thompson's Point and the open lake.

As the wind shifted from SE to NE approximately 3 hours after the release, however, the plume began to move SW. The strong NW winds recorded between hours 13 and 35 drove the peak dye concentration towards an area SE of McDonough Point, where it was observed on the second day of the experiment (hours 21-25) at a peak concentration of approximately .5 units, as shown in Figure 22. On the third day of the

study (44-46 hours), fluorescence ranged from .06-.07 units and no gradients could be detected.

Table 1 compares observed and predicted current speeds for the few hours of the experiment, based upon dye study results. At the surface, the maximum observed current velocity (based upon aerial photographs) was approximately 8 cm/sec, as compared with a predicted velocity of 1 cm/sec for the corresponding wind condition. Based upon movement of the peak dye concentration, the mean observed current velocity was approximately 1.7 cm/sec, as compared with a predicted mean velocity of .5 cm/sec.

Simulations of dye movement have also been performed using the linked hydrodynamic and transport models. Because each of these models assumes steady wind and current conditions and because wind conditions were variable during the dye study (Figure 21), it is necessary to break up the simulation into five periods of approximately uniform wind conditions, as indicated in Table 2. The root-mean-square wind speed (mixing energy input is proportional to square of wind speed) has been calculated for each period and used to drive the hydrodynamic model. An estimated speed of 5 mph has been assumed for periods with NE winds, since the Thompson's Point wind recording station is sheltered from NE winds. For comparison, simulations have also been performed using Burlington Airport data (at three-hour intervals) to drive the hydrodynamic and transport models.

Simulation results are compared with observed dye plume behavior in Figure 23. In this figure, each row corresponds to a different time period and each column, to a different simulation run or set of observed values. The parameters used for the four simulations are identical to those used in evaluations of hatchery impact (see **TRANSPORT MODEL REFINEMENTS**). For the first two runs, dispersion coefficients have been estimated by calibration against August-mid September 1984 phosphorus concentrations in the region. For the third and fourth runs, current patterns predicted by the hydrodynamic model have been used to drive the

transport model, based upon Thompson's Point and Burlington Airport wind measurements, respectively. The last column displays observed cell-mean concentrations, for each time period (corrected for a background fluorescence of approximately .1 units). The observed cell-mean values have been calculated from the dye contours (Figure 22) by area-weighted averaging within each cell. A scale factor of 10 is used to display observed and predicted concentrations in all cases.

Over the first 10 hours of the experiment, it is difficult to compare observed and predicted dye concentrations because the dye plume straddled cell boundaries and cells were not of uniform concentration, a condition which is inherent in the transport simulation. The comparisons are more valid at longer times (21 - 45 hrs). For both of these time periods, observed cell-mean dye concentrations and plume sizes were generally lower than modeled values for all simulation runs. Between 21 and 25 hours after the dye release, the center of the observed plume was somewhat further south (hugging the shoreline along McDonough Point) than predicted by the models, although observed concentrations (.1-.2 units) agree with model predictions. Generally, the simulations using the hydrodynamic model with Burlington Airport wind data show the best agreement with observed dye movements. Between 43 and 45 hours after the release, the models predict 4 to 15 cells exceeding .1 units, although no plume could be detected.

Consistent with drogue study results, dye study results suggest that current magnitudes in the region exceed those predicted by the hydrodynamic model. This under-estimation may be related to two factors: (1) under-estimation of the wind shear coefficient (a model parameter determining energy input at a given wind speed) and/or (2) under-estimation of effective wind speeds driving lake circulation. The above simulations (Figure 23) suggest that Burlington Airport data may be more representative of winds driving lake circulation than measurements made at Thompson's Point. Sheltering by land masses may be a significant problem at the latter station. The predicted current speeds assume that the land-based wind measurements are applicable to

the bays and open lake. Because of long fetches, wind speeds over the open lake are likely to be considerably higher than those measured on land. In order to resolve this issue, long-term monitoring of wind velocities over the open lake would be required. As they stand, however, the hydrodynamic and transport models are useful for generating conservative projections of hatchery impact, as indicated by the simulations of observed dye movements, discussed above, and by the simulations of observed phosphorus concentrations, discussed below.

TRANSPORT MODEL REFINEMENTS

This section describes refinements to the model previously employed for simulating spatial variations in phosphorus concentrations in the study region and for predicting hatchery impacts (Walker et al., 1986). Refinements have been made in the following areas:

(1) expansion of the hydrodynamic and transport grids (Figure 1) to include a total of 6,080 acres (vs. 3,960 acres included in previous version);

(2) improvements in communication between the hydrodynamic and transport model, including:
   (a) least-squares flow balancing;
   (b) estimation of exchange flows, as well as net advective flows between cells, based upon depth-integrated current velocities predicted by hydrodynamic model under a given wind condition.

(3) recalibration of the model (advective and diffusive versions) to August-mid September 1984 data.

(4) projection of hatchery impacts for effluent concentrations and flows specified in the draft discharge permit.

Results are discussed below.

Figure 24 displays phosphorus contours in the study region on ten sampling dates in 1984 (Smeltzer,1985). The proposed outfall (marked) is located in a region where contours tend to be relatively far apart, as compared with regions closer to the mouths of Lewis and Little Otter Creeks. The spacing of the contours and their general orientation in a NE-SW direction reflect circulation patterns in the region, as predicted by the hydrodynamic model. On most of the sampling dates, phosphorus concentrations in the vicinity of the outfall were more similar to those in the open lake west of Thompson's Point than to those in Hawkins Bay. The mixing regimes suggested by the observed phosphorus contours further support the selection of this outfall location.

Figure 24 also indicates that conditions in Hawkins and Town Farm Bays are influenced by the plume from Otter Creek (south of Kingsland Bay), as well as by loadings from Lewis and Little Otter Creek. The Otter Creek plume was particularly evident on June 27, July 26, August 17, September 7, September 19, and September 27. Given the general NE-SW current orientations, significant transport of phosphorus from the Otter Creek plume into Hawkins and Town Farm Bays may occur.

Previous modeling of phosphorus in the region (Smeltzer,1985; Walker et al.,1986) has focused on predicting average August-September conditions and has not explicitly accounted for effects of loadings from Otter Creek and for transport of phosphorus from the Otter Creek plume into the bays east of Thompson's Point. Figure 24 shows that Otter Creek plume was more evident and concentrations in the open lake west of Thompson's Point were generally higher on the last two sampling dates (September 19 and 27), as compared with other sampling dates in August and September. To reduce the influences of the Otter Creek plume and to improve the validity of the steady-state simulation, the transport model has been recalibrated against cell-average concentrations for the August 8, August 17, August 27, September 7, and September 13 sampling rounds.

The development of a least-squares flow balancing algorithm and estimation of exchange flows between cells based upon finite-element velocity fields represent significant improvements in the transport simulation. The distribution of wind load (squared mean daily speed) on direction for August-September 1984 is shown in Figure 25. Mixing energy input to the water column is clearly dominated by winds from the southeast. Application of the flow balancing algorithm to velocity fields predicted by the finite element model for a southeast wind results in the balanced flow velocities shown in Figure 26. Similar calculations have been performed using velocity fields generated by the hydrodynamic model for other wind directions (Figure 20). These are used in the subsequent section to evaluate the sensitivity of hatchery impacts to wind direction.

Tributary flows, concentrations, and loadings were higher during June and July, as compared with August and September of 1984. Previous modeling studies (Walker et al.,1986) have indicated that phosphorus residence time (ratio of mass in water column to external loading) is on the order of two weeks in the Hawkins and Town Farm Bay areas east of Thompson's Point. Some of the phosphorus measured in the water column during August and September 1984 reflects loadings which occurred earlier in the summer. To account for these effects, flows and loadings from Little Otter and Lewis Creeks have been calculated for the July 15-September 15 period and used in simulating water column concentrations between August and mid September.

Model variables and parameter estimates for phosphorus transport simulations are summarized in Table 3. Three approaches to modeling phosphorus transport have been investigated:

Case 1A: diffusive transport only, uniform dispersion coefficient;

Case 1B: diffusive transport only, different dispersion

coefficients for transport in north/south and east/west directions.

Case 2: diffusive transport + advective transport predicted by hydrodynamic model under dominant wind condition.

The first two approaches are empirical in that the dispersion coefficients must be calibrated against observed phosphorus concentrations. The third approach is less empirical because the lake currents predicted by the hydrodynamic model are the dominant transport mechanism and simulations are very insensitive to the assumed dispersion coefficient, as shown by the calibration curves in Figure 27. Consistent with earlier work (Walker, et al.,1986), dispersion coefficients have been calibrated against observed mean concentrations in the open bay and lake regions (away from shallow areas around creek mouths). Observed and predicted phosphorus concentrations for each Case are displayed in Figure 28.

The inclusion of Case 1B (different transport coefficients in the north/south vs. east/west directions) is based partially upon the balanced flow velocities predicted by the finite element model. As shown in Figure 26, the model predicts much higher exchange velocities in the open lake in the north/south direction (.8 cm/sec) vs. east/west direction (.1 cm/sec). As noted by Fischer et al. (1979), effective diffusivities in the direction of mean lake transport (south to north in this case) have been found to be an order of magnitude higher than diffusivities in a direction with is transverse to the mean transport. Because of the elongated shape of the lake and variations in wind fetch, effective eddy sizes may be larger for transport in the north/south vs. east/west directions; this, in turn, may have important implications for selection of appropriate diffusive transport coefficients (Okubo,1971; Walker,1985). As indicated by the calibration curves in Figure 27, Case 1B yields the lowest mean squared error for prediction of phosphorus concentrations (.62 vs. .74 for Case 2 and .76 for Case 1A). Several other combinations of north/south and east/west dispersion coefficients

have been investigated. A ratio of 5 (600,000 m^2/day to 120,000 m^2/day) yields the best fit, although other ratios (e.g., 10) work nearly as well.

For each Case, the model tends to over-predict phosphorus concentrations by 0-1 ppb in the open lake region west of Thompson's Point (Columns 11-14, Rows 4-9). It is possible that transport rates in this region are greater than those predicted by any of the above approaches. The models tend to under-predict phosphorus levels by 0-1 ppb in the southern portions of the bay (Columns 13-18, Rows 11-12). Intrusions from the Otter Creek plume and/or underestimation of tributary loadings may account for these small differences. Agreement between model simulations and observed phosphorus is generally good, especially considering the fact that the Case 2 predictions are based upon velocity fields which have been generated independently of the observed phosphorus data.

Simulations of the steady dye release conducted by Smelter(1985) during August and September of 1984 are shown in Figure 29. As found previously, the models calibrated for predicting phosphorus levels tend to over-predict measured dye concentrations resulting from the steady release. This may be related to non-conservative behavior of the dye over long time scales (e.g., adsorption to bottom sediments) and/or to under-prediction of lake currents.

HATCHERY IMPACT PROJECTIONS

Drogue studies and simulations of phosphorus and dye distributions in 1984 and 1986 support the validity of the linked hydrodynamic and transport models as tools for developing conservative projections of hatchery impact. The models are used below to evaluate the sensitivity of hatchery impacts to location, discharge concentration, wind direction, and wind speeds.

Hatchery impact projections for each Case under August loading conditions (effluent concentration = 90 ppb) are illustrated in Figure 30. The impacts are expressed as increases in cell phosphorus concentration (ppb) attributed to the hatchery discharge. A plot scale factor of 10 has been used to enhance resolution. Increases for other months can be estimated in proportion to the hatchery effluent concentration (ranging from 86 to 111 ppb, Table 3). The August loading condition is most representative of impacts during the critical algal growth period. The advective model predicts a maximum increase of 2.1 ppb in the hatchery discharge cell and increases of 1.7-1.9 ppb throughout the bay areas east of Thompson's Point. The diffusive models predict greater impacts within the discharge cell (2.5-3 ppb), but similar increases throughout most of the bay (1.7-2.1 ppb).

As discussed previously (Walker et al.,1986), bay-wide increases are probably of greater significance from a water quality perspective than increases within the discharge cell because low residence time in the discharge cell would limit algal responses to the increased nutrient levels. The models do not account for currents and dilution induced by the diffuser and therefore likely over-estimate phosphorus increases in the discharge cell. Generally, the impact projections on bay-wide conditions are relatively insensitive to choice of model (advective vs. diffusive).

Sensitivities of impacts to wind direction under August loading conditions are illustrated in Figure 31. Because of variability in direction and speed and because of the appreciable residence time of phosphorus in the bay, it is unlikely that conditions would ever equilibrate with any fixed wind regime. The simulations in Figure 31 are intended to show general directions of changes in relation to wind direction. These simulations show that projected impacts are greater for the southeast and northwest wind directions than for the others. The above projections for the dominant southeast wind event likely overestimate the impacts, when shifting wind directions are considered.

Impact sensitivities to the combined effects of variations in wind speed, direction, and hatchery loading are shown in Figure 31. Time series of daily mean wind speed and direction at Burlington Airport for June-September 1984 have been used to develop 122 sets of daily current patterns. These, in turn, have been used to drive the transport model in a dynamic mode in order to predict spatial and temporal variations in phosphorus over the 122-day period, as induced by the hatchery discharge at 11.5 mgd and effluent concentrations at the proposed monthly limits (Table 3). Average wind speed for June-September 1984 was 8.2 mph, in relation to the 30-year mean of 7.9 mph for the same months. Initial values for the simulation (June 1) have been set at the steady-state solution under the dominant wind event (SE, 8.5 mph).

Time series of hatchery impacts at six locations in the bay are shown in Figure 31. As expected, the impacts are greatest and most variable in the discharge cell. As discussed above, the model likely over-predicts increases and variability within the discharge cell because effects of currents induced by the diffuser at not considered. Increases of less than 4 ppb are predicted in the discharge cell under worst-case conditions (generally following a day or two of low wind speeds). At locations further distant from the discharge cell, the level and variability of the hatchery impact decreases. This reflects increased volume and a greater sensitivity to average wind conditions, as opposed to daily conditions. When these variations are considered, the range of impacts is generally between 1 and 2 ppb throughout most of the bay areas east of Thompson's Point, as reflected by the dashed lines in Figure 23.

Under the proposed effluent limitations, the projected mean impact of the hatchery on phosphorus levels east of Thompson's Point is less than 2 ppb. This conclusion is similar to that reached based upon earlier versions of the hydrodynamic and transport models (Figure IV-11, p. 56, Case 2, Mean Flow, Effluent P = 100 ppb, Walker et al., 1986). This change ~~should be~~ should be evaluated in relation to:

(1) 5 ppb average increase set by the Vermont Department of Water Resources as an acceptable level of impact;

(2) observed temporal variations in phosphorus concentrations in the open waters of the bay under existing conditions (range 12-25 ppb, see Figure 24), as induced by fluctuations in loadings from Little Otter, Lewis, and Otter Creeks, mixing characteristics, and other physical, chemical, and biological factors;

(3) observed year-to-year variations in average phosphorus concentrations at the longterm lay monitoring station off Thompson's Point (range 11-21 ppb, 1979-1984 means, Walker,1986);

(4) observed temporal variations in transparency off Thompson's Point (ranging seasonally from 2 to 8 meters);

(5) spatial variations in Lake Champlain, in particular the south-north gradient which ranges from 56 to 10 ppb, based upon 1979-1985 monitoring data (Walker,1986).

Analyses of phosphorus, chlorophyll-a, and transparency data from throughout Lake Champlain (Walker,1986) indicate that nuisance algal growths (defined as chlorophyll-a concentrations exceeding 20 ppb or transparencies less than 2 meters) are generally not found at detectable frequencies in waters with total phosphorus concentrations less than 25-30 ppb. An increase from 15 to less than 17 ppb in the average phosphorus concentration east of Thompson's Point is not likely to result in nuisance algal densities and will maintain a mesotrophic classification for the bay.

CONCLUSIONS

(1) An outfall location 400 meters west of Gardiner Island is favorable for minimizing local water quality effects of the hatchery discharge. Discharge through a diffuser will take advantage of the 1.7-9.3 cm/sec currents measured during the drogue and dye studies under prevailing winds and will minimize the potential for localized increases in nutrient concentrations during periods of low winds.

(2) Phosphorus contours observed during 1984 indicate that water quality in the vicinity of the proposed outfall is more similar to the open lake waters west of Thompson's Point than to the shallow Hawkins Bay area. This is consistent with favorable currents in the area. The orientation of phosphorus contours is also consistent with the dominant SW-NE current patterns predicted by the hydrodynamic model under prevailing SE winds.

(3) An outfall location further out into the main lake would result in a discharge to the hypolimnion. A location closer to the hatchery and McDonough Point would place the discharge in a region where current velocities tend to be higher, but where a higher percentage of the effluent would be transported through shallow regions of Hawkin's Bay under dominant wind regimes.

(4) Comparisons of measured and modeled current velocities indicate that the hydrodynamic model used to project hatchery impacts captures the general structure of circulation patterns in the region, but generally under-predicts current magnitudes, when driven by wind measurements taken at Thompson's Point. Underestimation of effective wind speeds driving lake circulation and/or the effective wind shear

coefficient may contribute to differences between observed and predicted current magnitudes.

(5) Simulations of observed dye movements following release at the outfall location on September 15, 1986 also indicate that actual current velocities and local dilution potential exceed those predicted by the hydrodynamic and transport models. The best agreement between model simulations and observed dye movements is obtained when Burlington Airport wind measurements are used to drive lake circulation. Sheltering of the Thompson's Point wind station may limit the usefulness of the data for simulating lake currents.

(6) Drogue studies and simulations of phosphorus and dye distributions in 1984 and 1986 support the validity of the linked hydrodynamic and transport models as tools for developing conservative (i.e., worst-case) projections of hatchery impact.

(7) Under the proposed effluent limitations, the discharge will cause an increase of 1-2 ppb in the bay waters east and south of Thompson's Point under summer conditions. This conclusion is largely insensitive to modeling assumptions (advective vs. diffusive transport), wind direction, and typical seasonal variability in wind speeds. This conclusion is also consistent with projections developed from earlier versions of the hydrodynamic and transport models (Walker et al., 1986).

(8) The projected 1-2 ppb increase in phosphorus concentration is within the maximum 5 ppb increase which has been determined by the Vermont Department of Water Resources as an acceptable level of impact. Based upon comparisons with other sources of spatial and temporal variability in the system, the effects of a 1-2 ppb increase in phosphorus on water quality and water uses will be difficult to detect. Phosphorus concentrations

in the bay will remain well below levels which are required to support nuisance phytoplankton growths, based upon review of data from other regions of Lake Champlain.

REFERENCES

Fischer, J.B., E.J. List, R.C.Y. Koh, J. Imberger, and N.H. Brooks, Mixing in Inland and Coastal Waters, Academic Press, New York, 1979.

Okubo, A., "Oceanic Diffusion Diagrams", Deep-Sea Research, Vol. 18, pp. 789-802, 1971.

Smeltzer, E., "Lake Champlain Fish Hatchery Discharge Study", Vermont Department of Water Resources and Environmental Engineering, 1985.

Walker, W.W., "Documentation for P2D and S2D: Software for Analysis and Prediction of Water Quality Variations in Two Dimensions", prepared for Vermont Department of State Buildings and Vermont Department of Water Resources and Environmental Engineering, April 1985.

Walker, W.W., J.P. Laible, E.M. Owens, and S.W. Effler, "Impact of an Offshore Hatchery Discharge on Phosphorus Concentrations in and Around Hawkins Bay, Lake Champlain", prepared for State of Vermont, Department of Fish and Wildlife, March 1986.

Walker, W.W., "Perspectives on Eutrophication in Lake Champlain", prepared for Department of Fish and Wildlife, June 1986.

LIST OF TABLES

Table 1

Comparison of Measured and Modeled Currents

August 18, 1986 Drogue Study
Wind Direction = NNW Speed = 13.8 mph

DEPTH (m)	MEASURED (cm/s)	MODELED (cm/s)
1	12.8	6.6
3	5.2	3.4
6	3.8	3.4

August 28, 1986 Drogue Study
Wind Direction = N Speed = 5-13 mph

DEPTH (m)	MEASURED (cm/s)	MODELED (cm/s)
1	7.3	4.2
3	3.9	2.3
6	7.6	1.5
9	8.5	1.5

September 2, 1986 Drogue Study
Wind Direction = NW Speed = 5-10 mph

DEPTH (m)	MEASURED (cm/s)	MODELED (cm/s)
1	3.0	2.0
3	3.0	0.3
6	3.0	1.2

September 3, 1986 Drogue Study
Wind Direction = SSE Speed = 9.3 mph

DEPTH (m)	MEASURED (cm/s)	MODELED (cm/s)
1	14.8	3.6
3	12.2	1.9
6	9.6	1.2
8	9.3	1.4

September 15, 1986 Dye Study 0-5 hrs
Wind Direction = SE Speed = 4.5 mph

DEPTH	MEASURED (cm/s)	MODELED (cm/s)	
Surface	8.0	1.0	(from aerial photo)
Mean	1.7	0.5	(from dye measurements)

Table 2

Time Periods and Wind Conditions
for Dye Study Simulations

	Time(hrs)			Speed
Period	Start	Stop	Direction	mph
1	0	3.6	SE	4.3
2	3.6	9.4	NW	5.4
3	9.4	15.4	NE	5.0
4	15.4	39.4	NW	8.8
5	39.4	56.0	NE	5.0

Table 3
Simulation Variables and Parameters

Tributary Inputs	Flow m3/day	Phosphorus Conc. ppb	
Lewis + Little Otter	58,000	68	July 15-Sept 15, 1984
Thorp and Kimball	2,400	68	"
Hatchery	43,569	(see below)	
Open Lake Throughflow	3,200,000	12	Aug-Sept 1984, Col. 13
Open Lake Throughflow	3,800,000	12	Aug-Sept Mean, Col. 13

Phosphorus Decay Rate = .001 day^{-1}
Atmospheric Loading = .055 mg/m^2-day

Dye Loading (Aug-Sept 1984) = 87 grams/day, (Col 18, Row 13)
Dye Effective Settling Velocity (Photochemical Decay) = .091 m/day

Hatchery Permit Concentrations
(Including 15 ppb Background for Kingsland Bay Intake)

Month	Conc(ppb)
June	103
July	86
August	90
Sept	111

	Dispersion Coef.(m^2/day) East-West	North-South	Aug-Sept 1984 Phos. Error Mean Square
Case 1A	140,000	140,000	.76
Case 1B	120,000	600,000	.62
Case 2	10,000	10,000	.74

Advective Transport - Case 2
Dominant Wind Direction: SE
Effective Wind Speed: 8.55 mph
= Root Mean Square Daily Mean Speed, Burlington Airport, August-September 1984

LIST OF FIGURES

Figure 1
Location Map and Expanded Simulation Grid

Cell Width = 400 meters

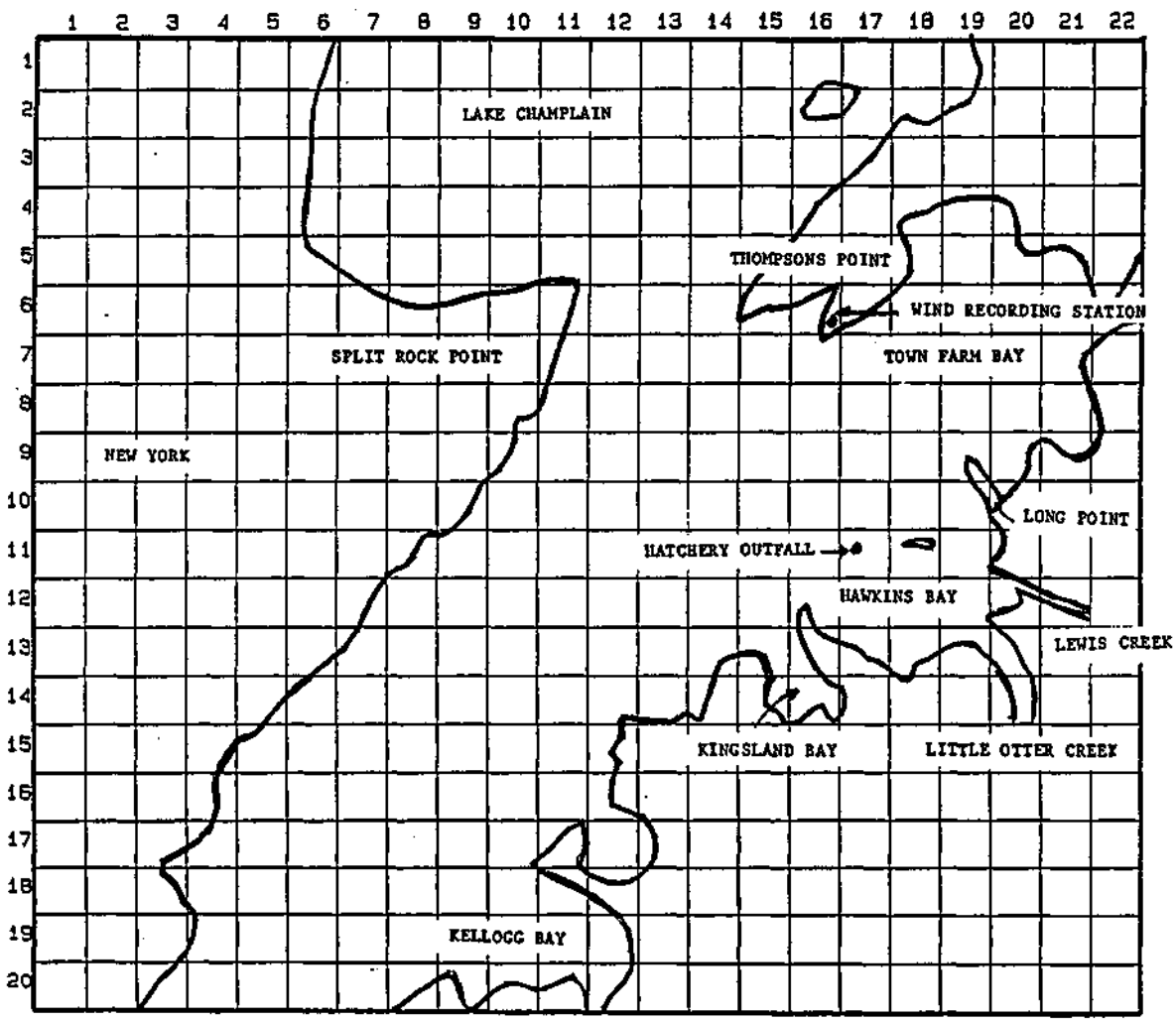

Figure 2

Wind Rose - Thompson's Point
September 1986

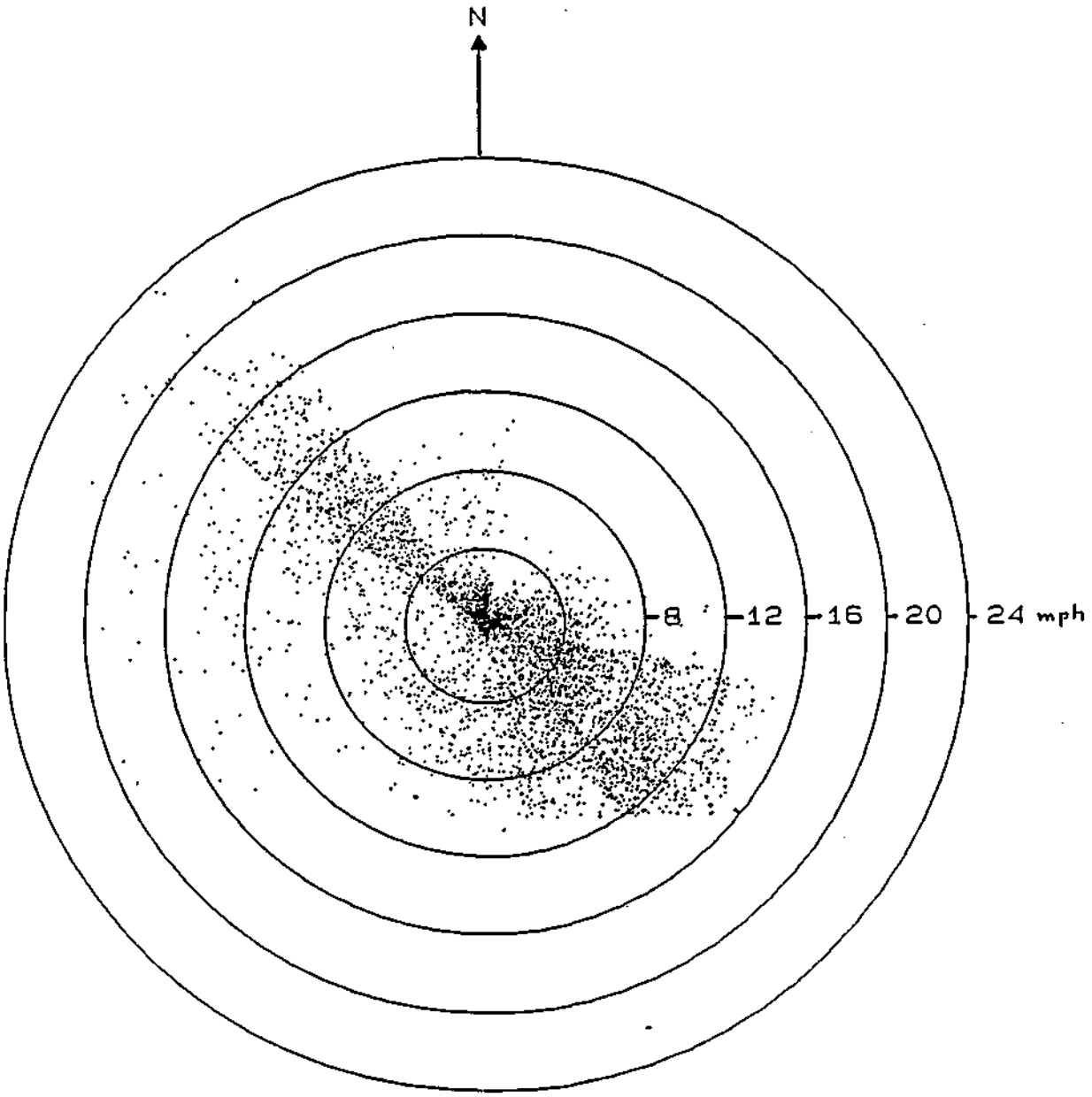

Figure 3

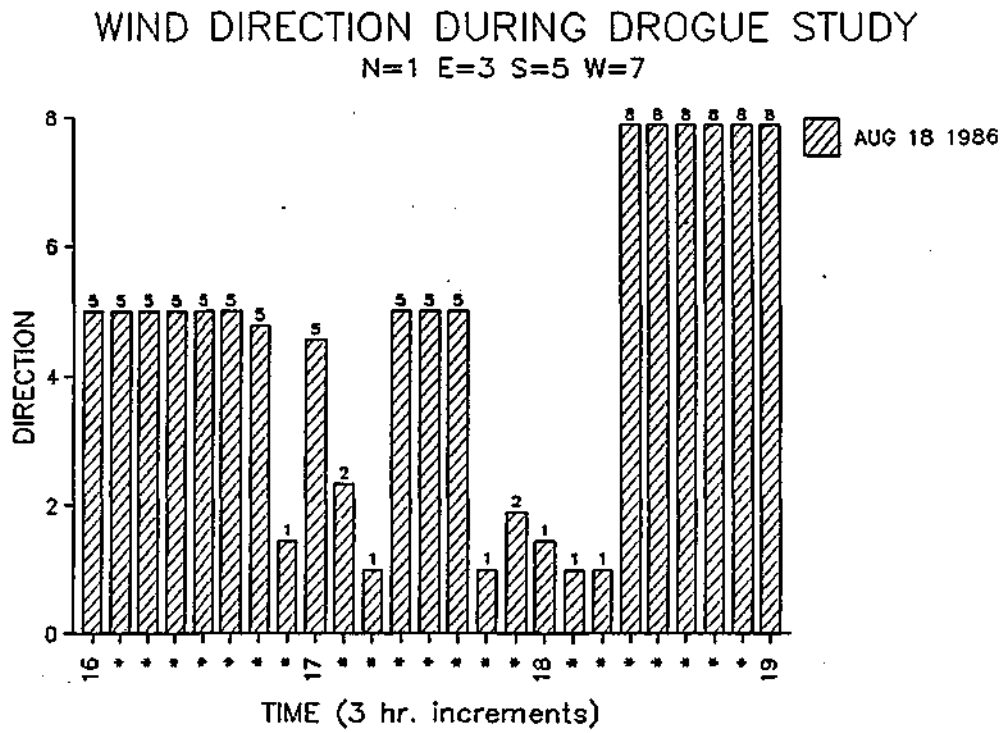
WIND DIRECTION DURING DROGUE STUDY
N=1 E=3 S=5 W=7
AUG 18 1986
DIRECTION
TIME (3 hr. increments)

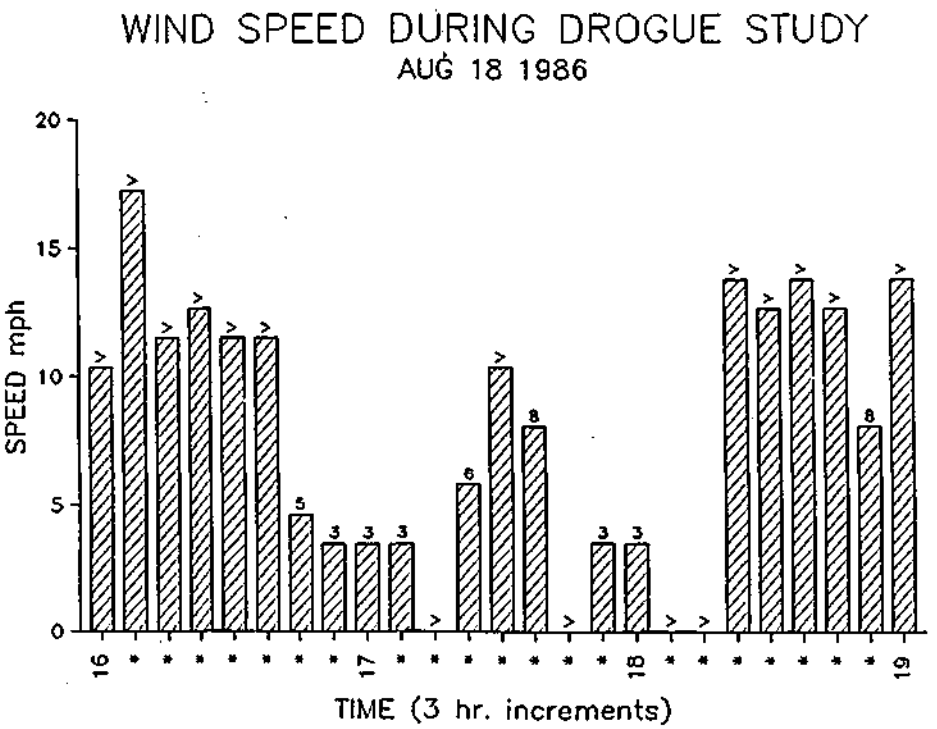
WIND SPEED DURING DROGUE STUDY
AUG 18 1986
SPEED mph
TIME (3 hr. increments)

Figure 4

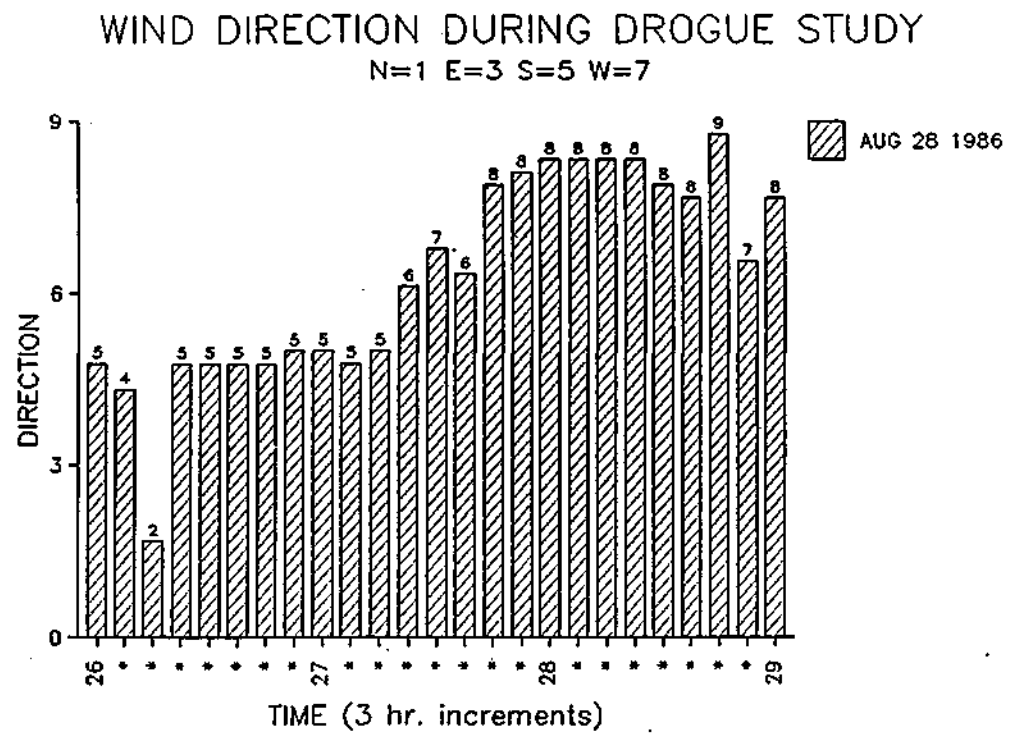
WIND DIRECTION DURING DROGUE STUDY
N=1 E=3 S=5 W=7
AUG 28 1986
DIRECTION
TIME (3 hr. increments)

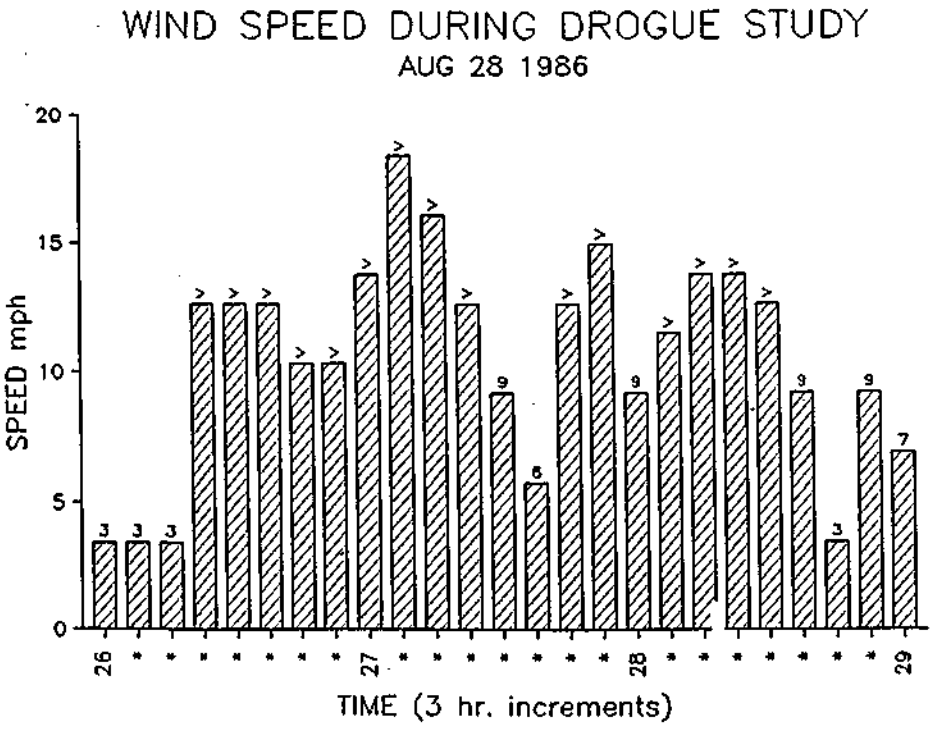
WIND SPEED DURING DROGUE STUDY
AUG 28 1986
SPEED mph
TIME (3 hr. increments)

Figure 5

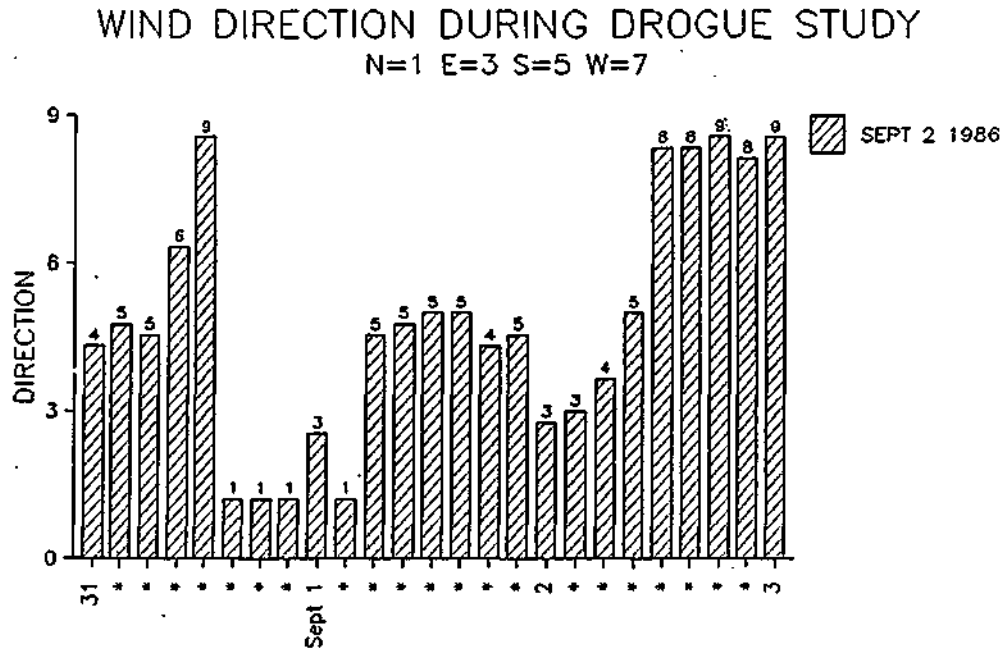
WIND DIRECTION DURING DROGUE STUDY
N=1 E=3 S=5 W=7
SEPT 2 1986
DIRECTION
TIME (3 hr. increments)

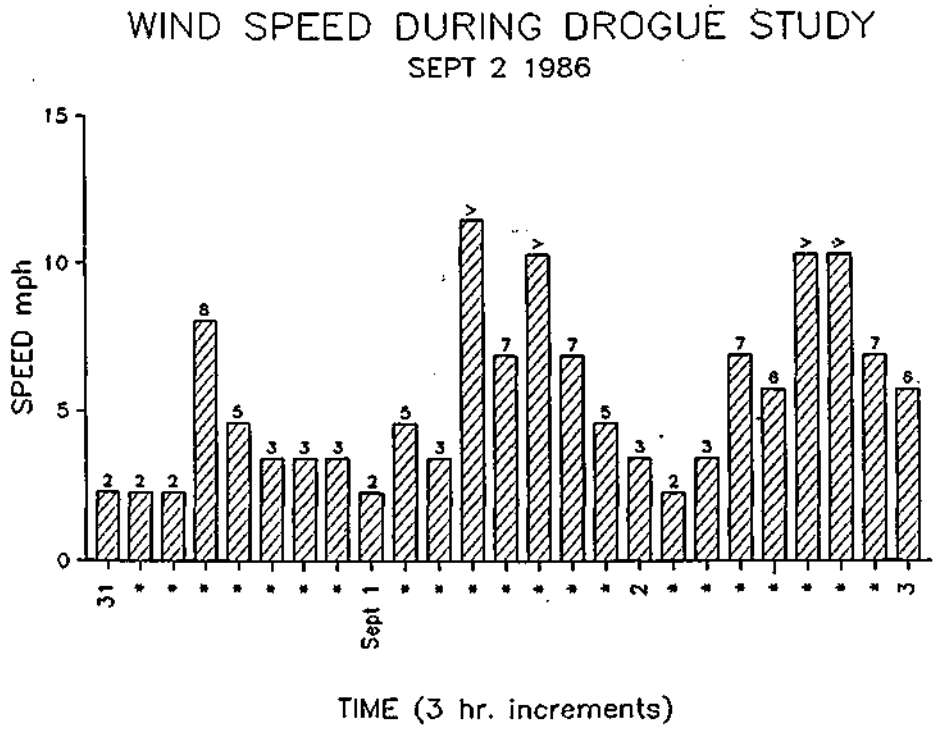
WIND SPEED DURING DROGUE STUDY
SEPT 2 1986
SPEED mph
TIME (3 hr. increments)

Figure 6

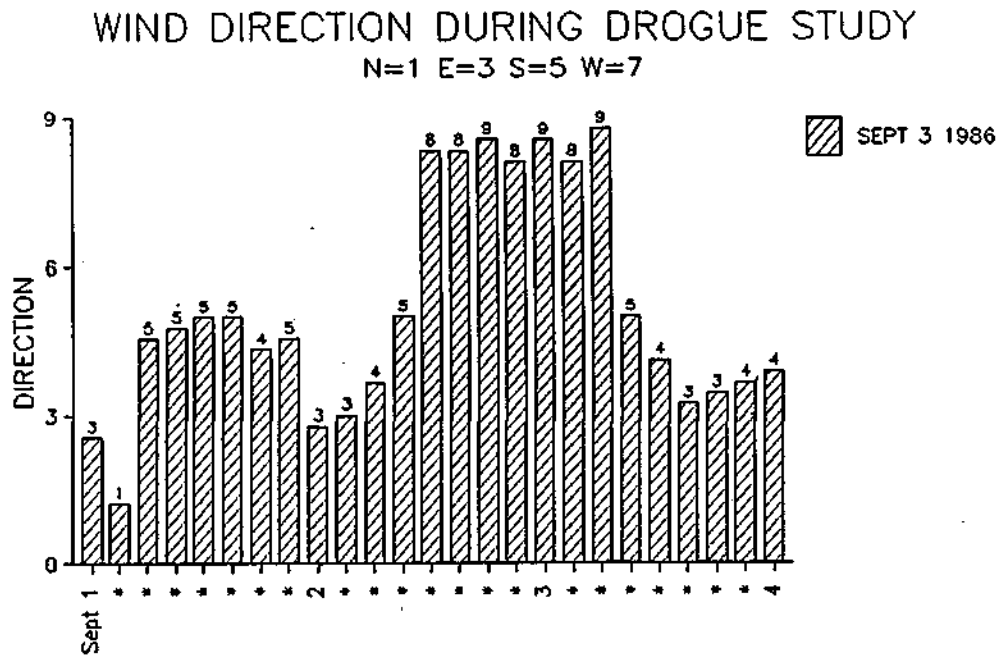
WIND DIRECTION DURING DROGUE STUDY
N=1 E=3 S=5 W=7
SEPT 3 1986
DIRECTION
0
3
6
9
Sept 1
2
3
4
TIME (3 hr. increments)

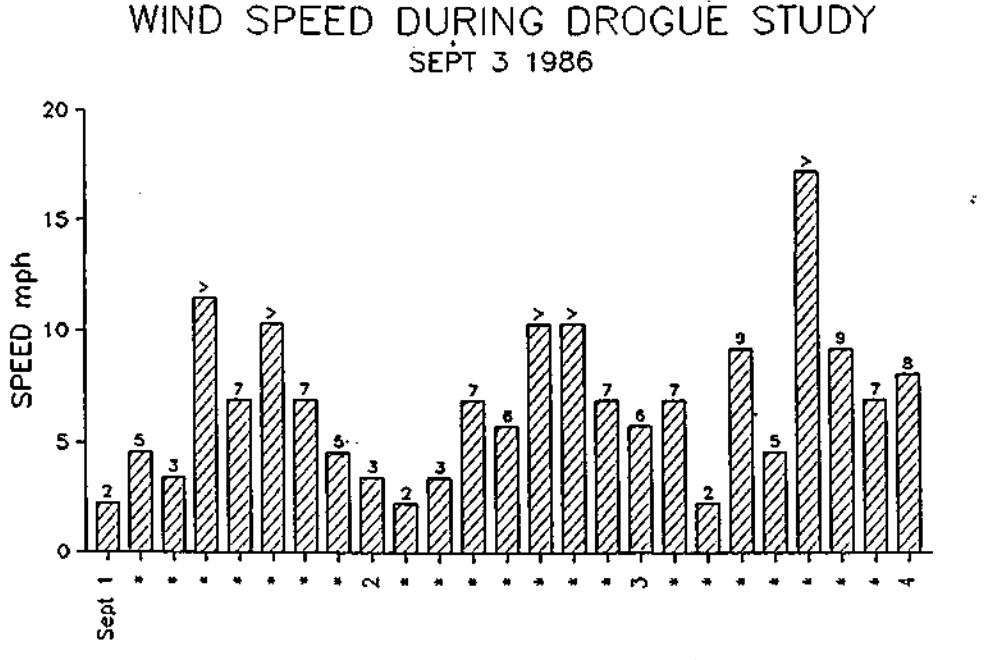
WIND SPEED DURING DROGUE STUDY
SEPT 3 1986
SPEED mph
0
5
10
15
20
Sept 1
2
3
4
TIME (3 hr. increments)

Figure 7

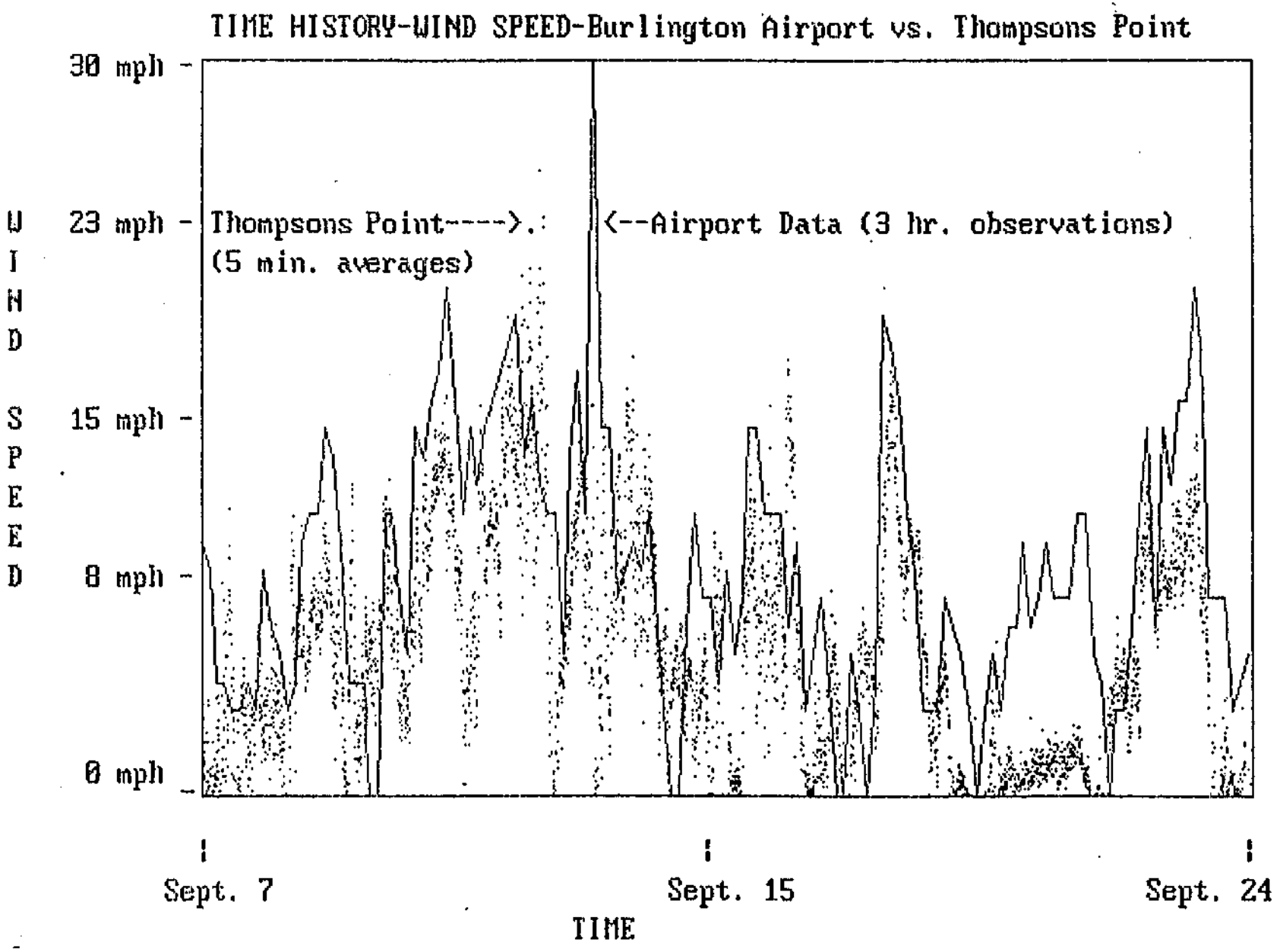
TIME HISTORY-WIND SPEED-Burlington Airport vs. Thompsons Point
30 mph
23 mph
15 mph
8 mph
0 mph
WIND SPEED
Thompsons Point---->.:
(5 min. averages)
<--Airport Data (3 hr. observations)
Sept. 7
Sept. 15
Sept. 24
TIME

Figure 8

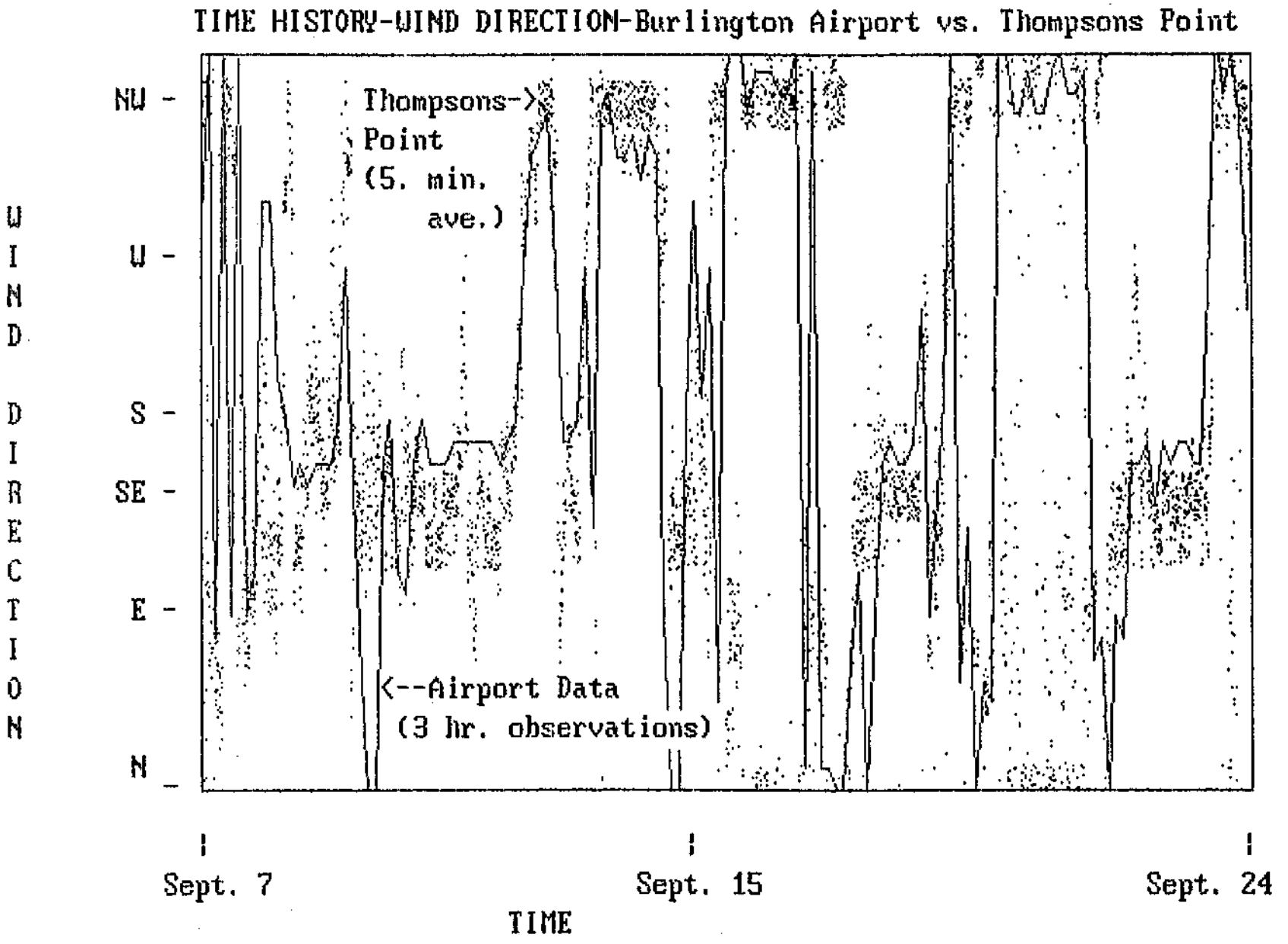
TIME HISTORY-WIND DIRECTION-Burlington Airport vs. Thompsons Point
NW
W
S
SE
E
N
WIND DIRECTION
Thompsons-> Point (5. min. ave.)
<--Airport Data (3 hr. observations)
Sept. 7
Sept. 15
Sept. 24
TIME

Figure 9

Wind Direction Histograms
Four Categories

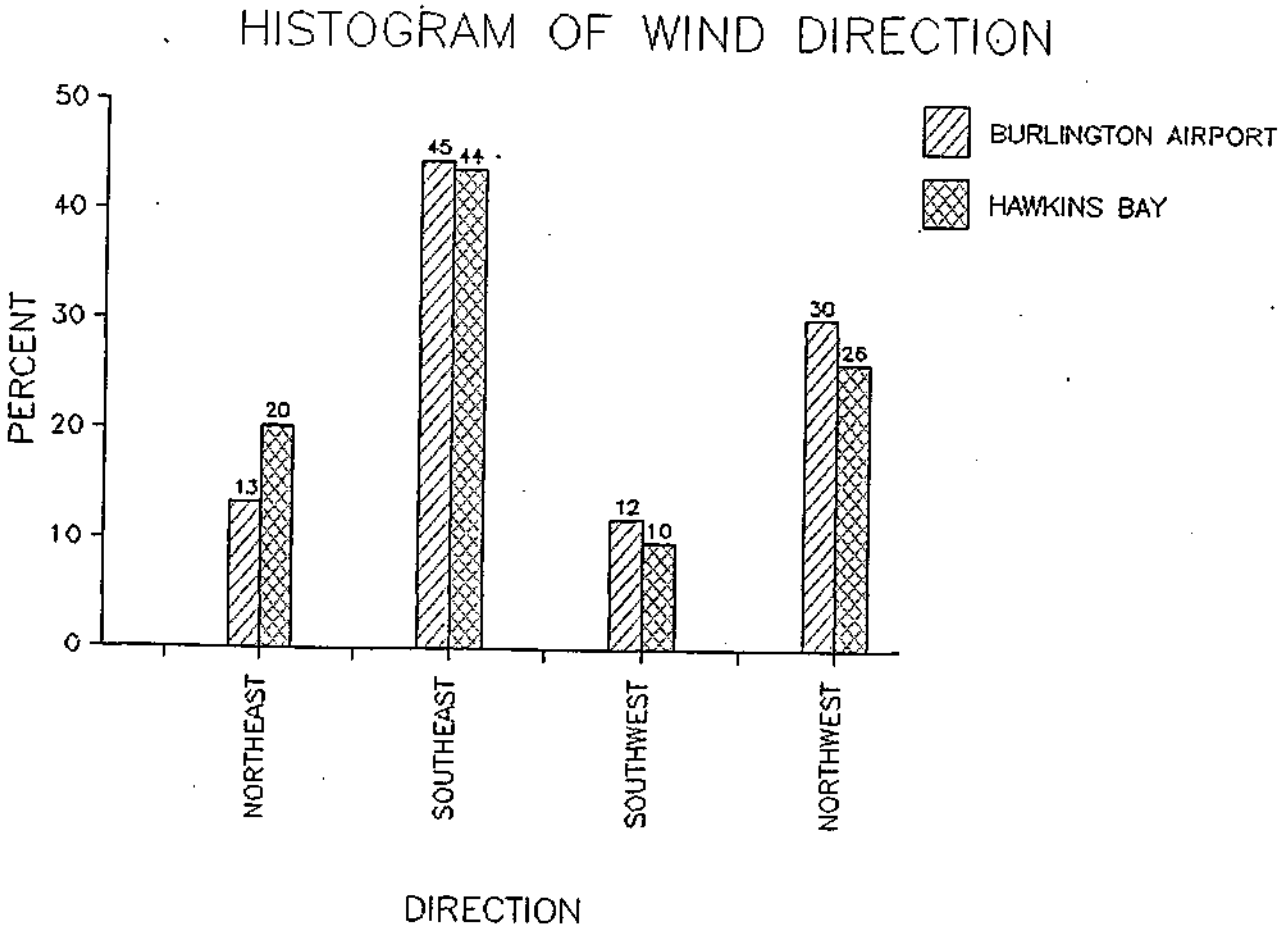

Figure 10

Wind Direction Histograms
Eight Categories

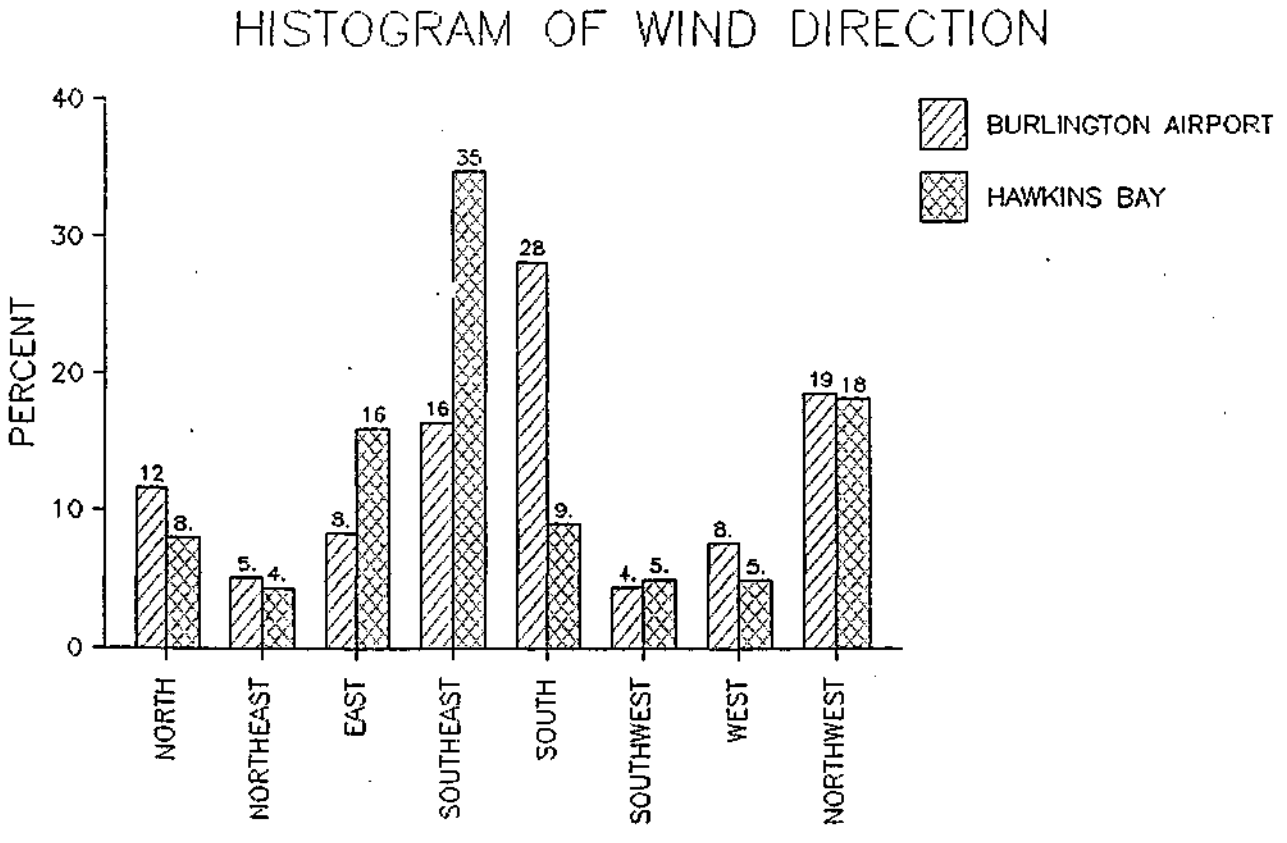

Figure 11

Drogue Study Results

Date	Wind	Mean Current Speed (cm/sec) Surface	Bottom
1 August 18, 1986	NNW 10-15 mph	9.0	3.8
2 August 28, 1986	NNE 5-13 mph	7.3	10.6
3 September 2, 1986	NW 5-10 mph	2.4	2.0
4 September 3, 1986	SSE 5-10 mph	13.5	9.4

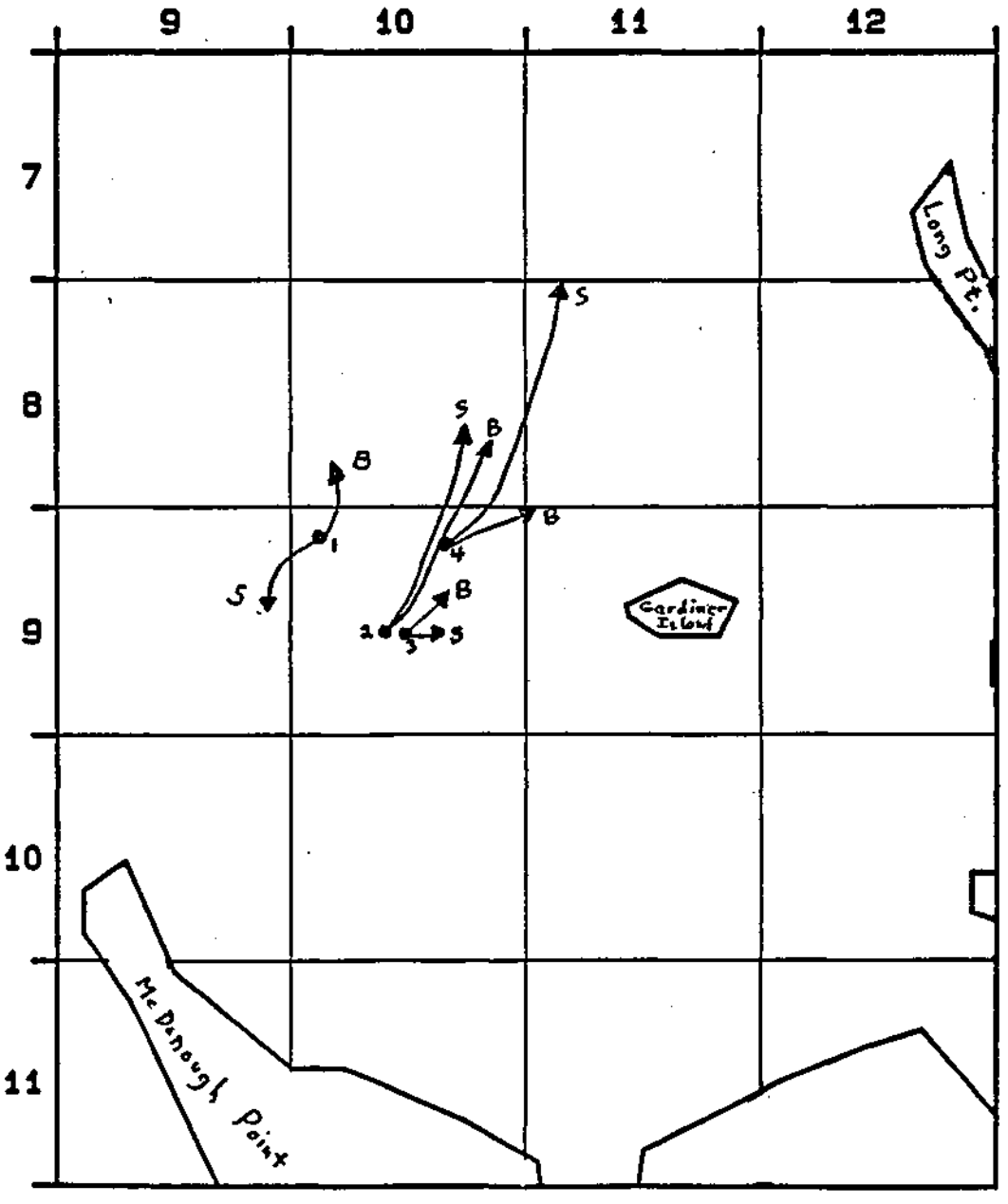

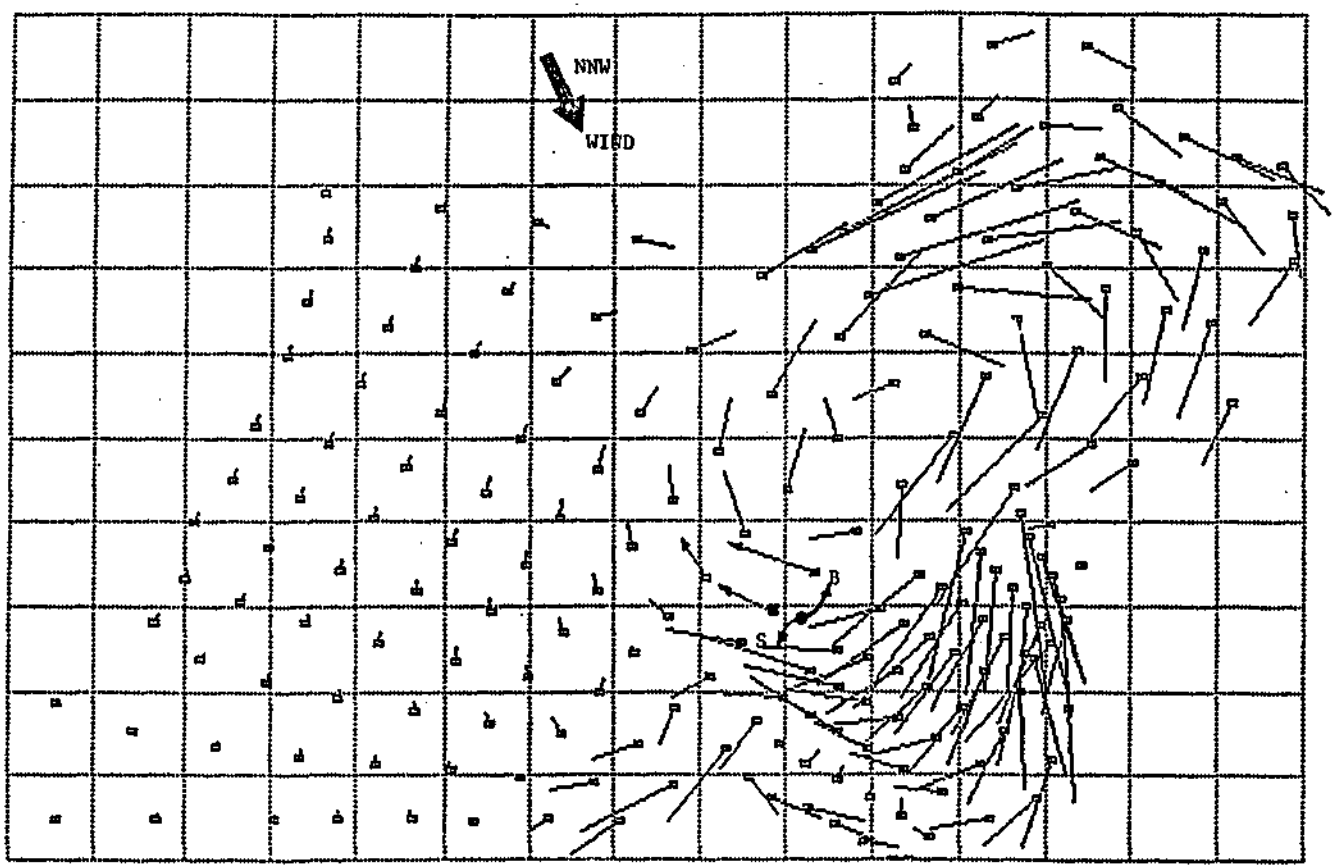

Figure 12

● Release Point

▲ Node 82

Scale Units
0 1 2 3

Vertically Averaged Velocity Vectors
From Computer Simulation
and
Measured Drogue Paths
Wind Conditions NNW, W_{mean} = 13.8 mph

August 18, 1986

S = Surface Current
B = Bottom Current

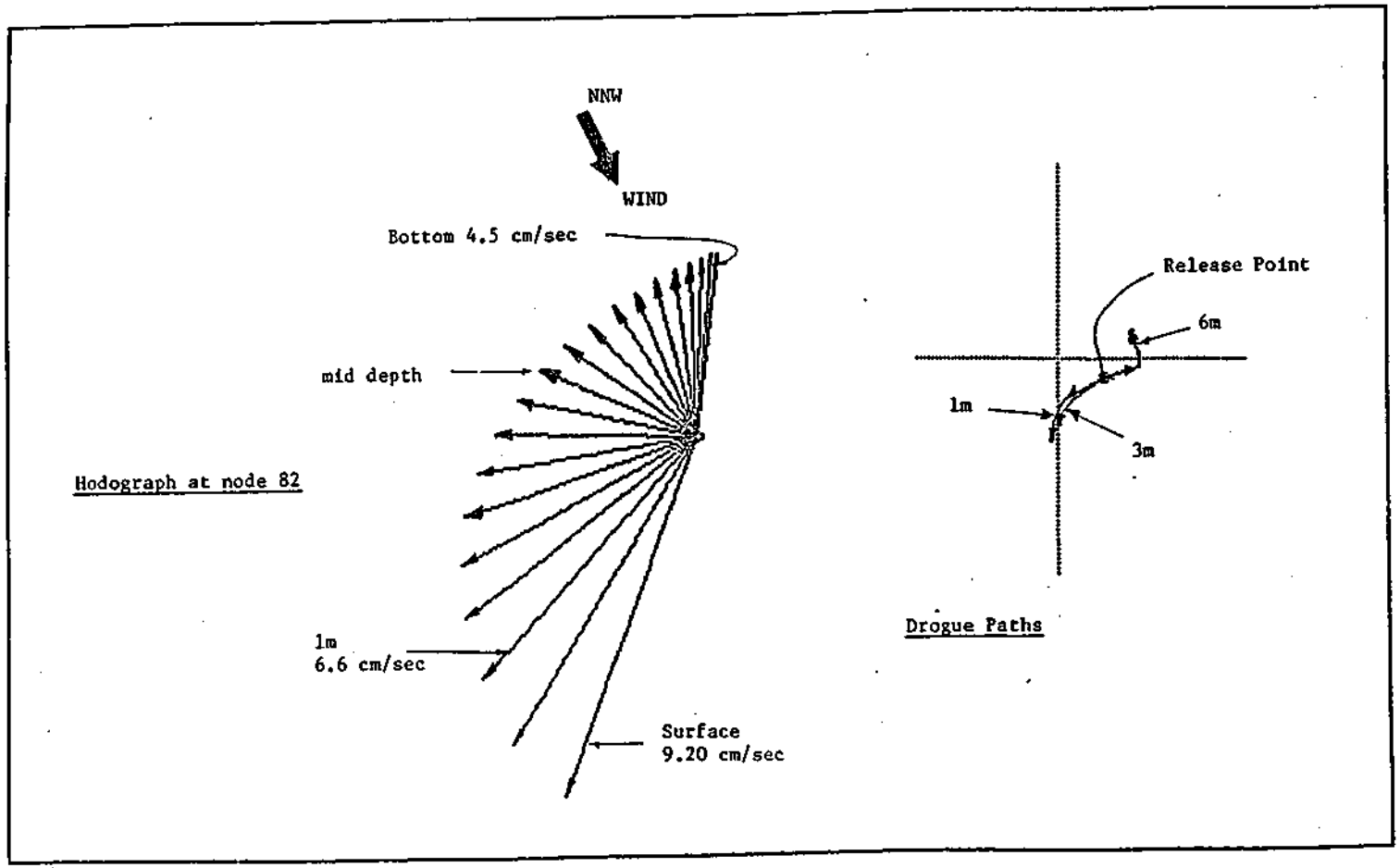

Figure 13

Measured Drogue Paths and Simulated Flow Hodograph
Wind Condition NNW, W_{mean} = 13.8 mph

August 18, 1986

Figure 14

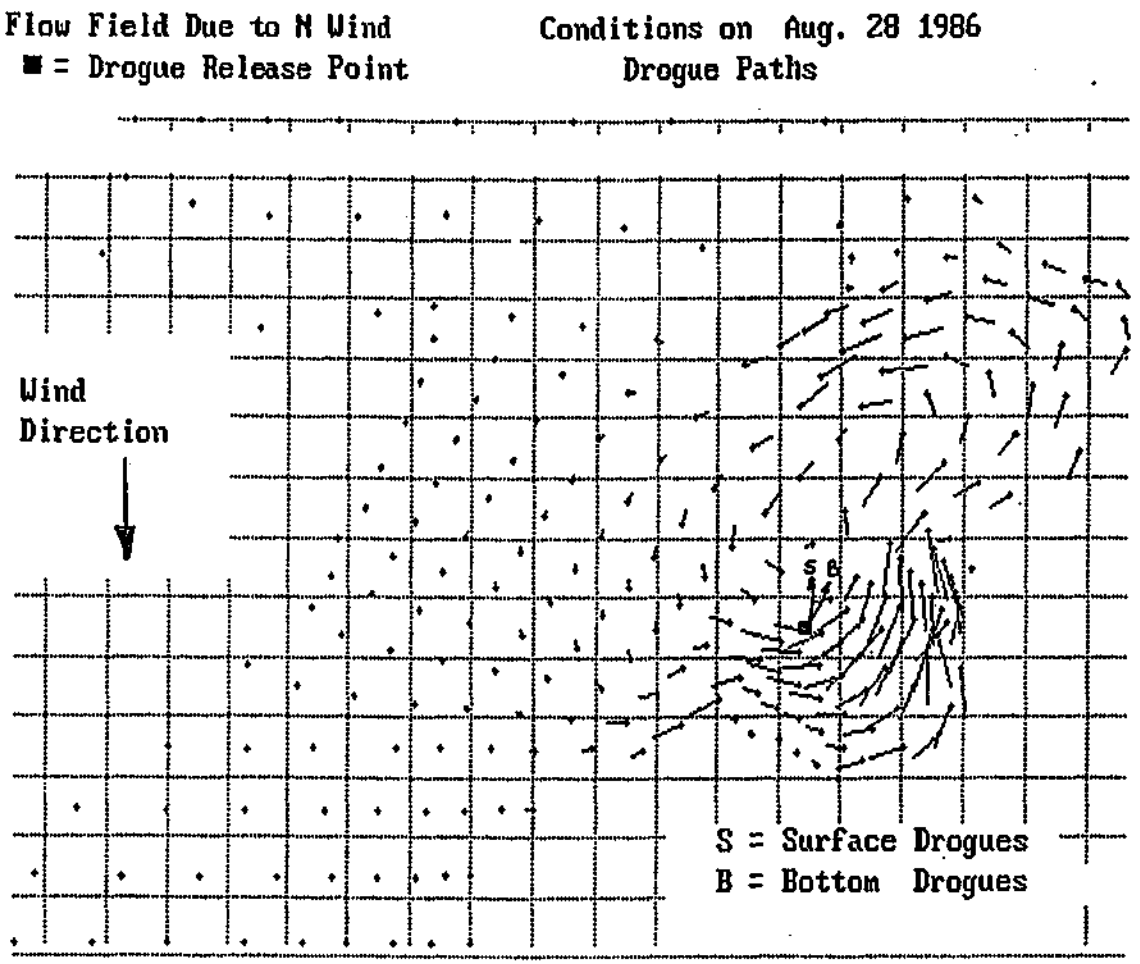
Flow Field Due to N Wind
■ = Drogue Release Point
Conditions on Aug. 28 1986
Drogue Paths
Wind
Direction
S B
S = Surface Drogues
B = Bottom Drogues

Figure 15

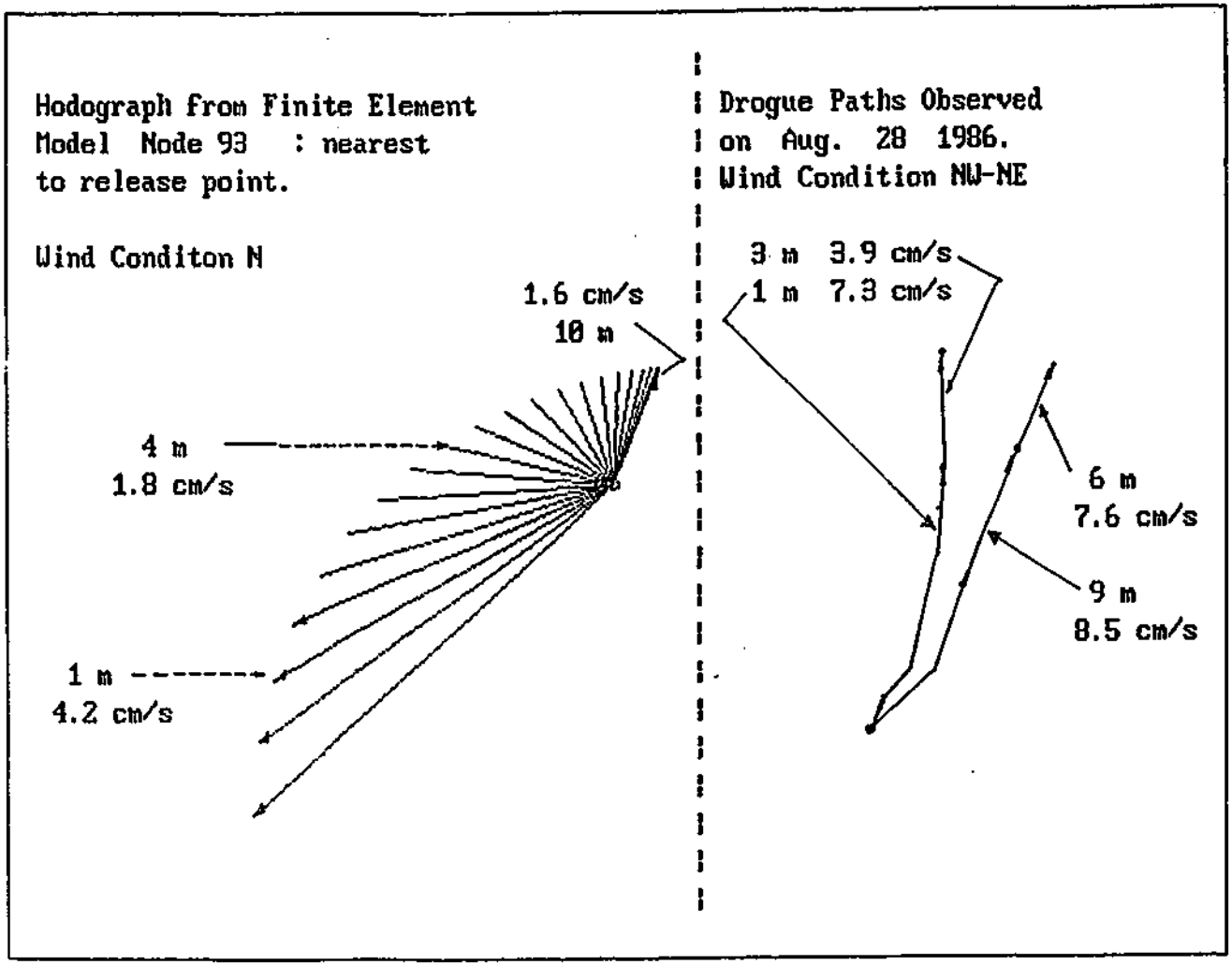
Hodograph from Finite Element
Model Node 93 : nearest
to release point.
Wind Conditon N
1.6 cm/s
10 m
4 m
1.8 cm/s
1 m
4.2 cm/s
Drogue Paths Observed
on Aug. 28 1986.
Wind Condition NW-NE
3 m 3.9 cm/s
1 m 7.3 cm/s
6 m
7.6 cm/s
9 m
8.5 cm/s

Figure 16

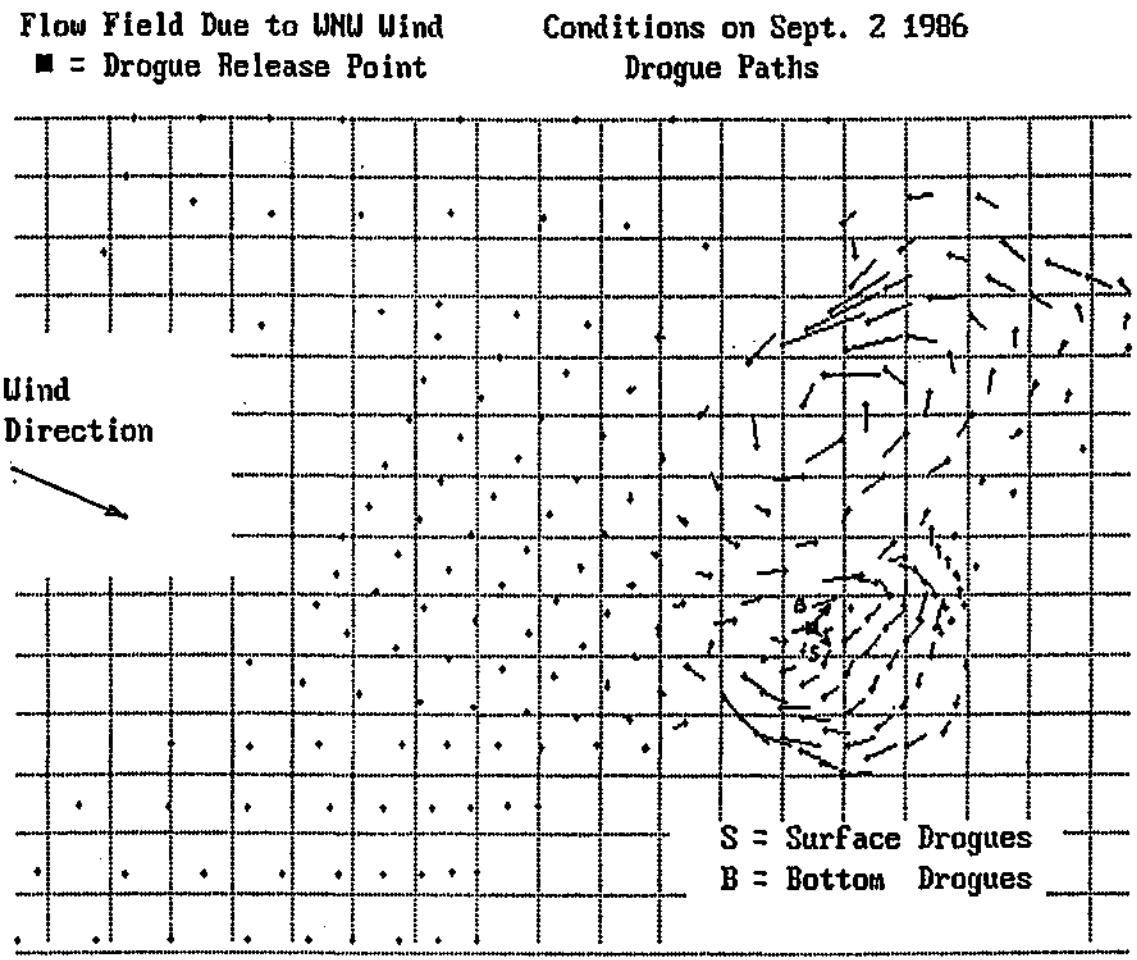
Flow Field Due to WNW Wind
■ = Drogue Release Point
Conditions on Sept. 2 1986
Drogue Paths
Wind
Direction
S = Surface Drogues
B = Bottom Drogues

Figure 17

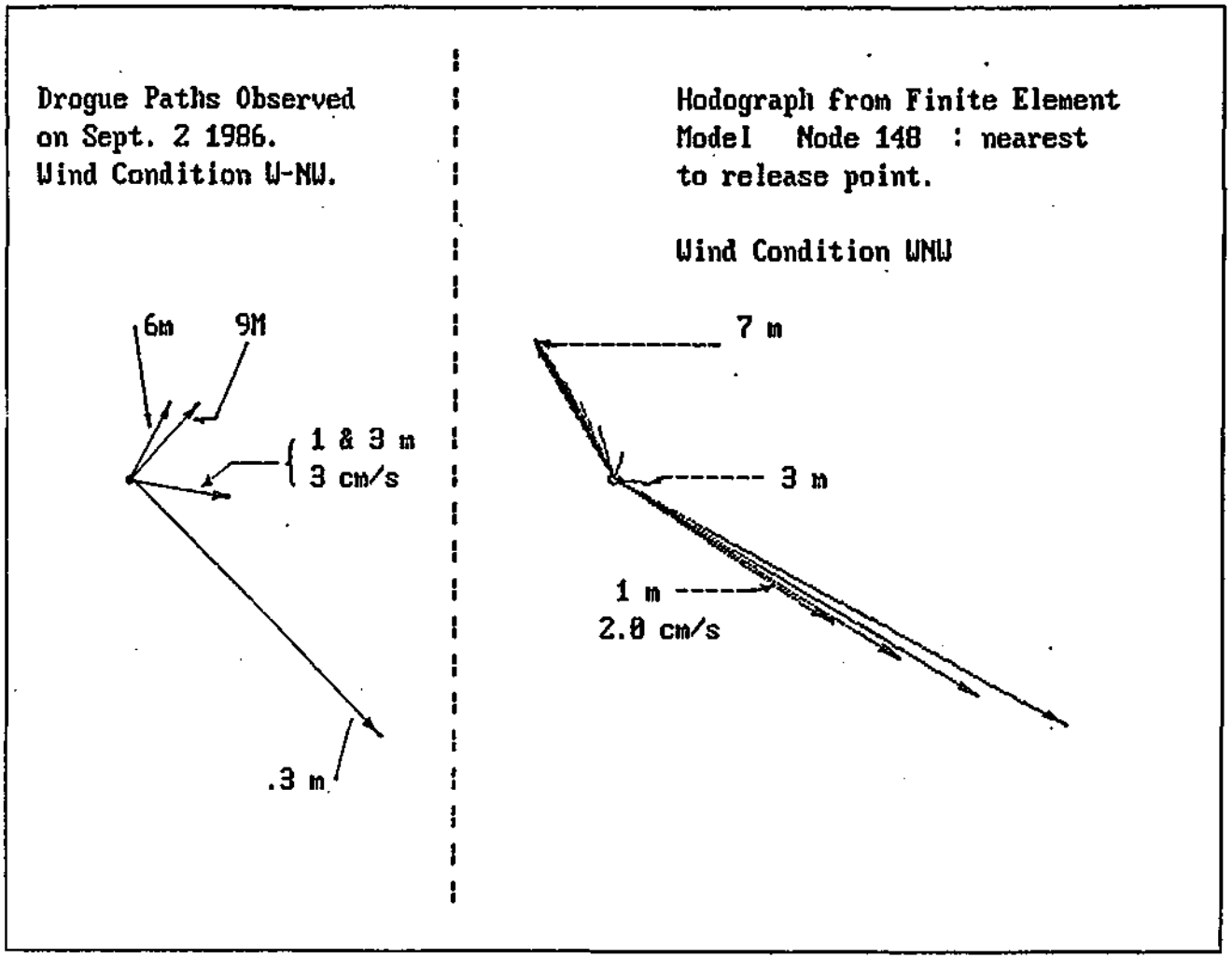
Drogue Paths Observed
on Sept. 2 1986.
Wind Condition W-NW.
6m
9M
1 & 3 m
3 cm/s
.3 m
Hodograph from Finite Element
Model Node 148 : nearest
to release point.
Wind Condition WNW
7 m
3 m
1 m
2.0 cm/s

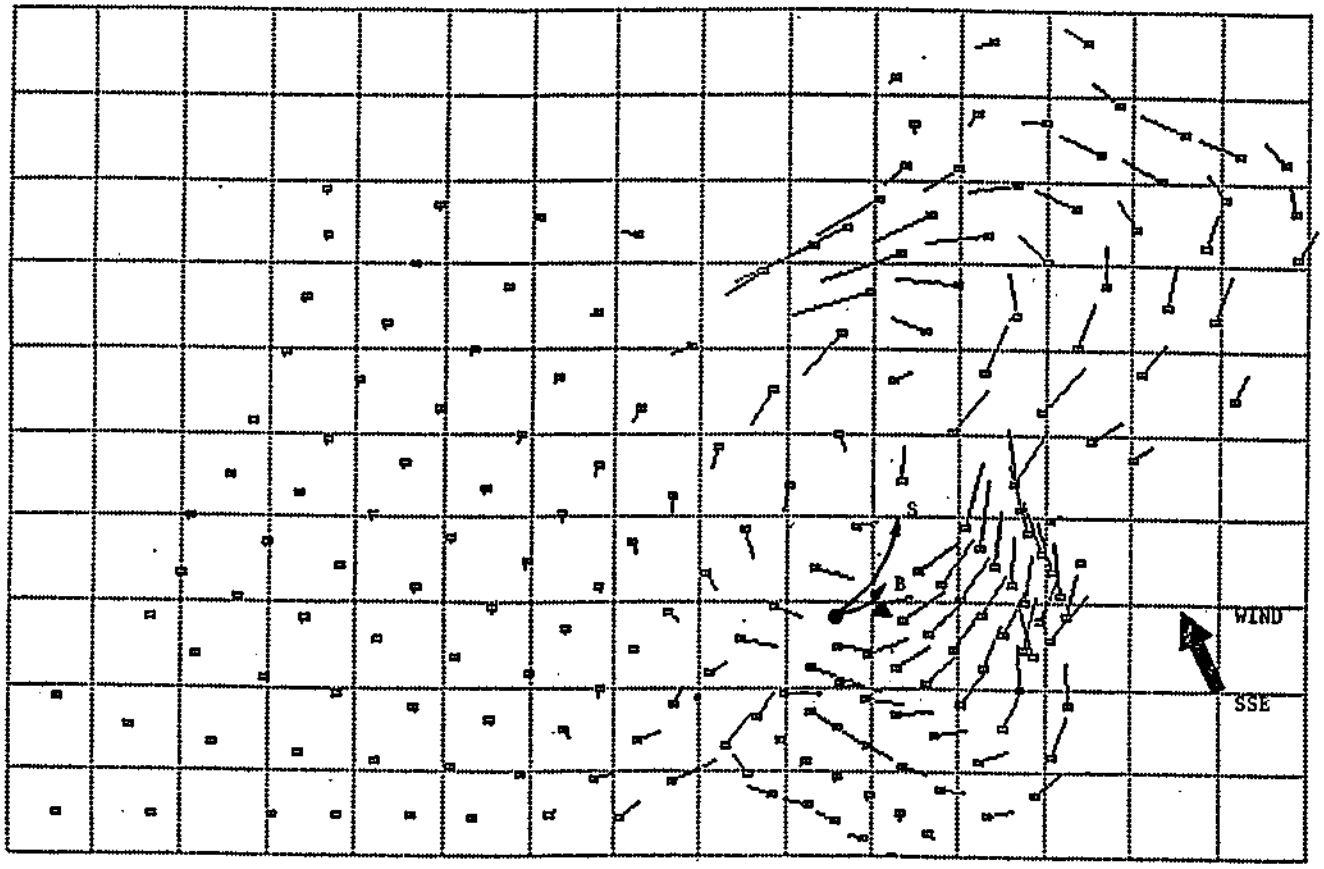

Figure 18

Vertically Averaged Velocity Vectors
From Computer Simulation
and
Measured Drouge Paths
Wind Condition SSE, W_{mean} = 9.3 mph

September 3, 1986

● Release Point

▲ Node 92

Scale cm/s
0 1 2 3

S = Surface Current
B = Bottom Current

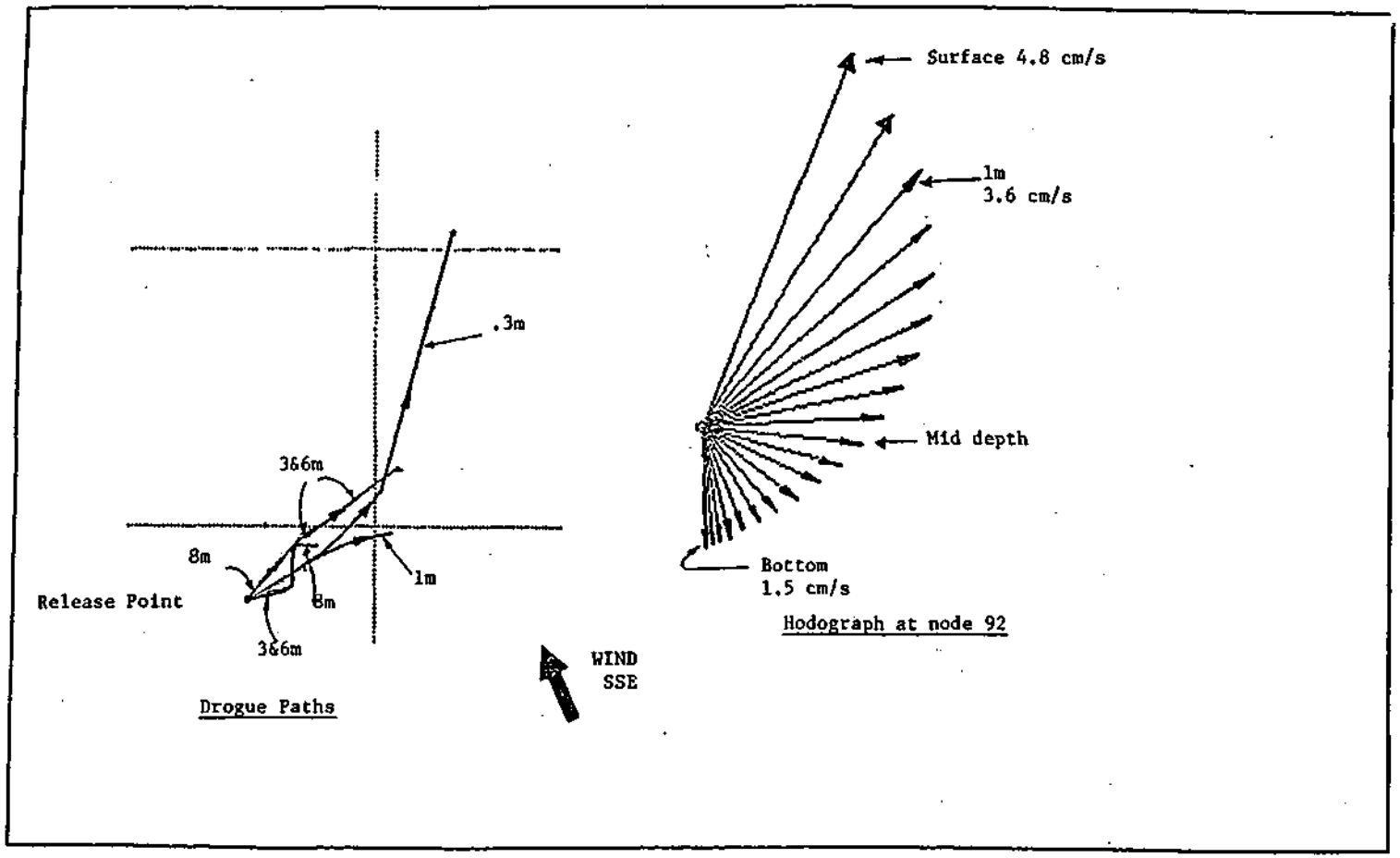

Figure 19

Measured Drogue Paths and Simulated Flow Hodograph
Wind Condition SSE, W_{mean} = 9.3 mph

September 3, 1986

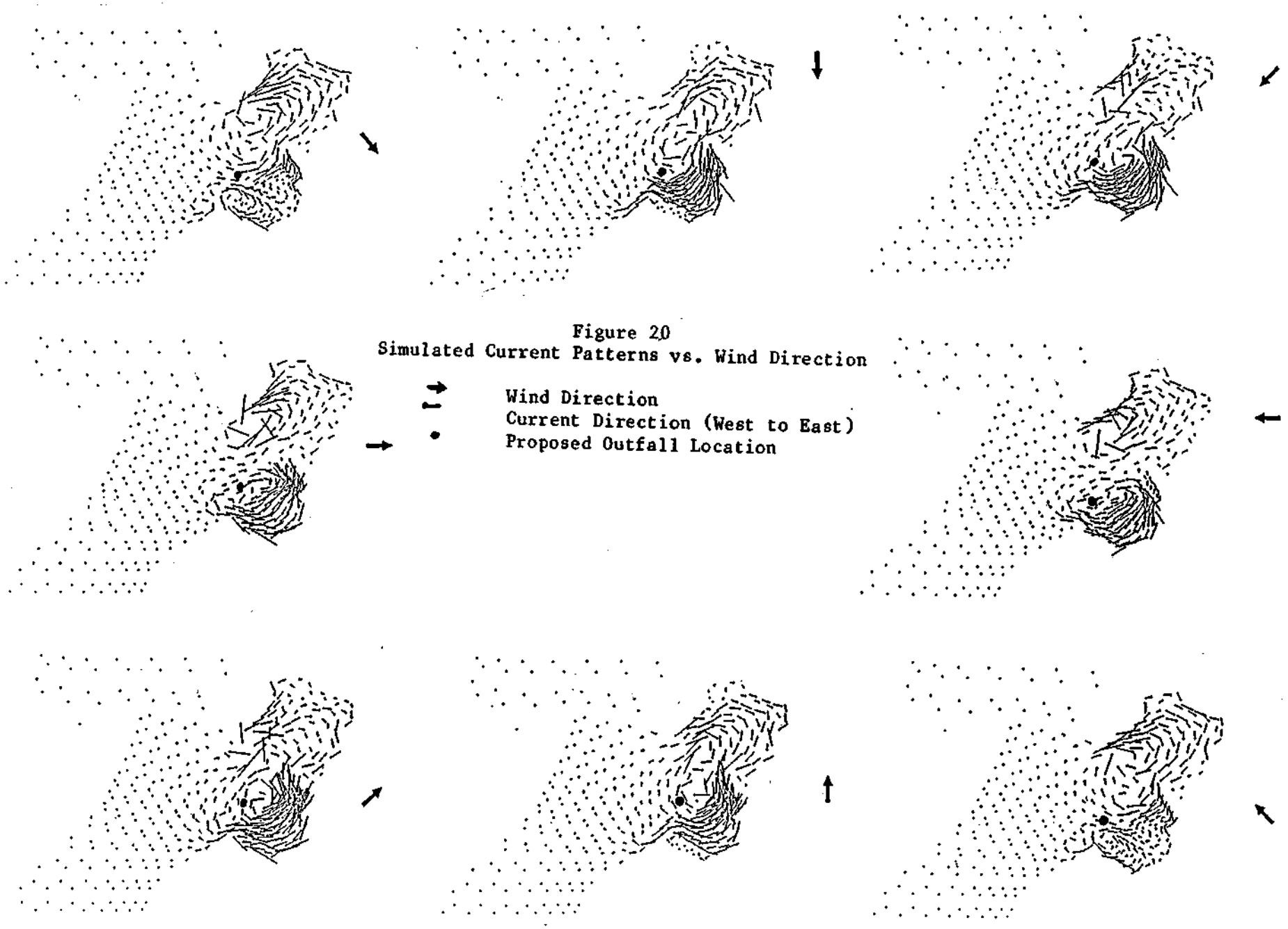

Figure 20
Simulated Current Patterns vs. Wind Direction

Figure 21

Wind Velocities During Dye Study

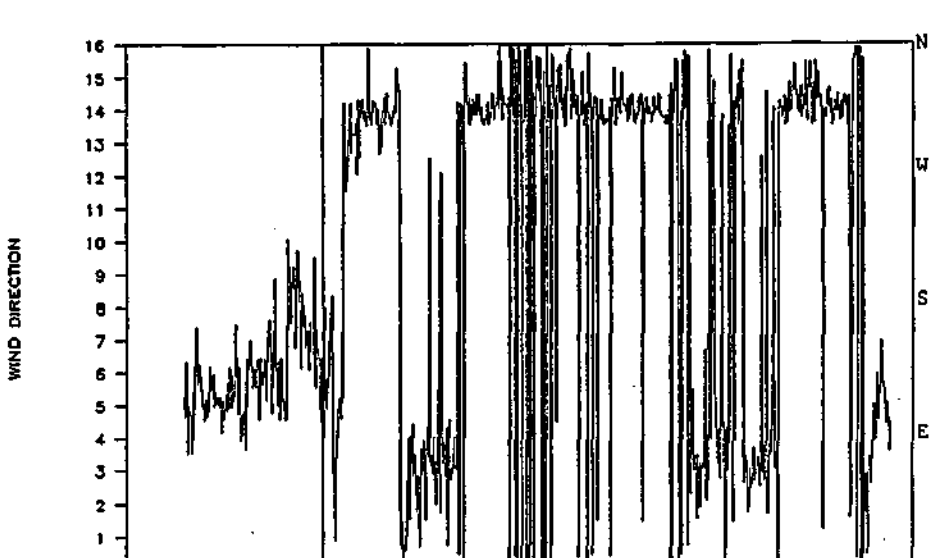

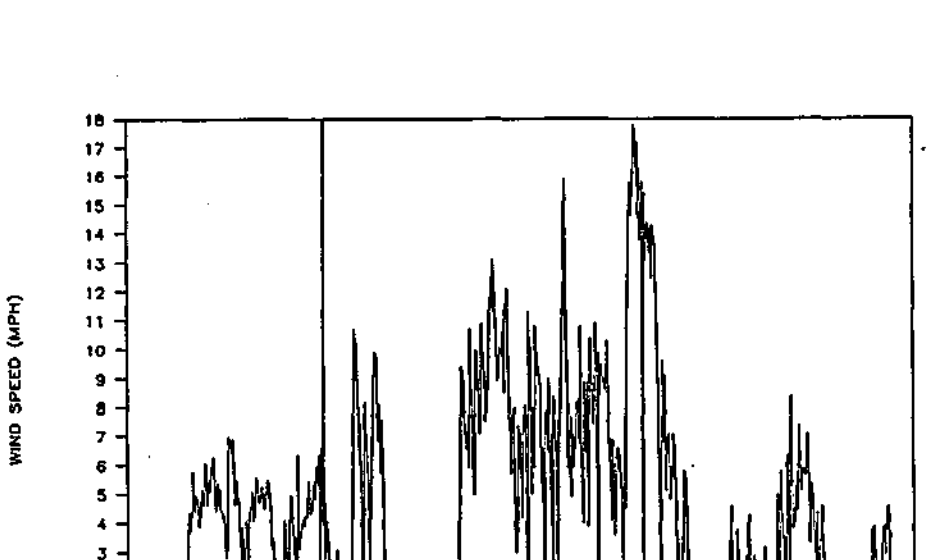

Figure 22
Observed Dye Behavior
September 15-17, 1986

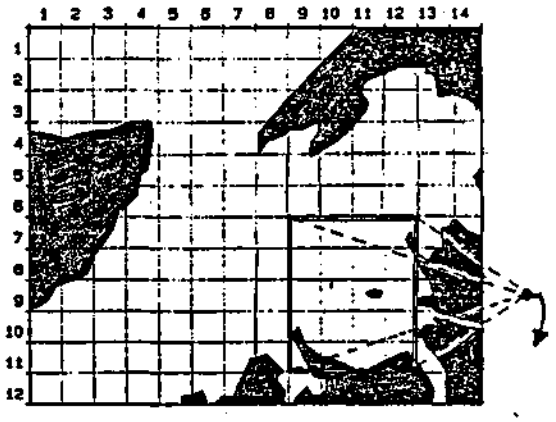

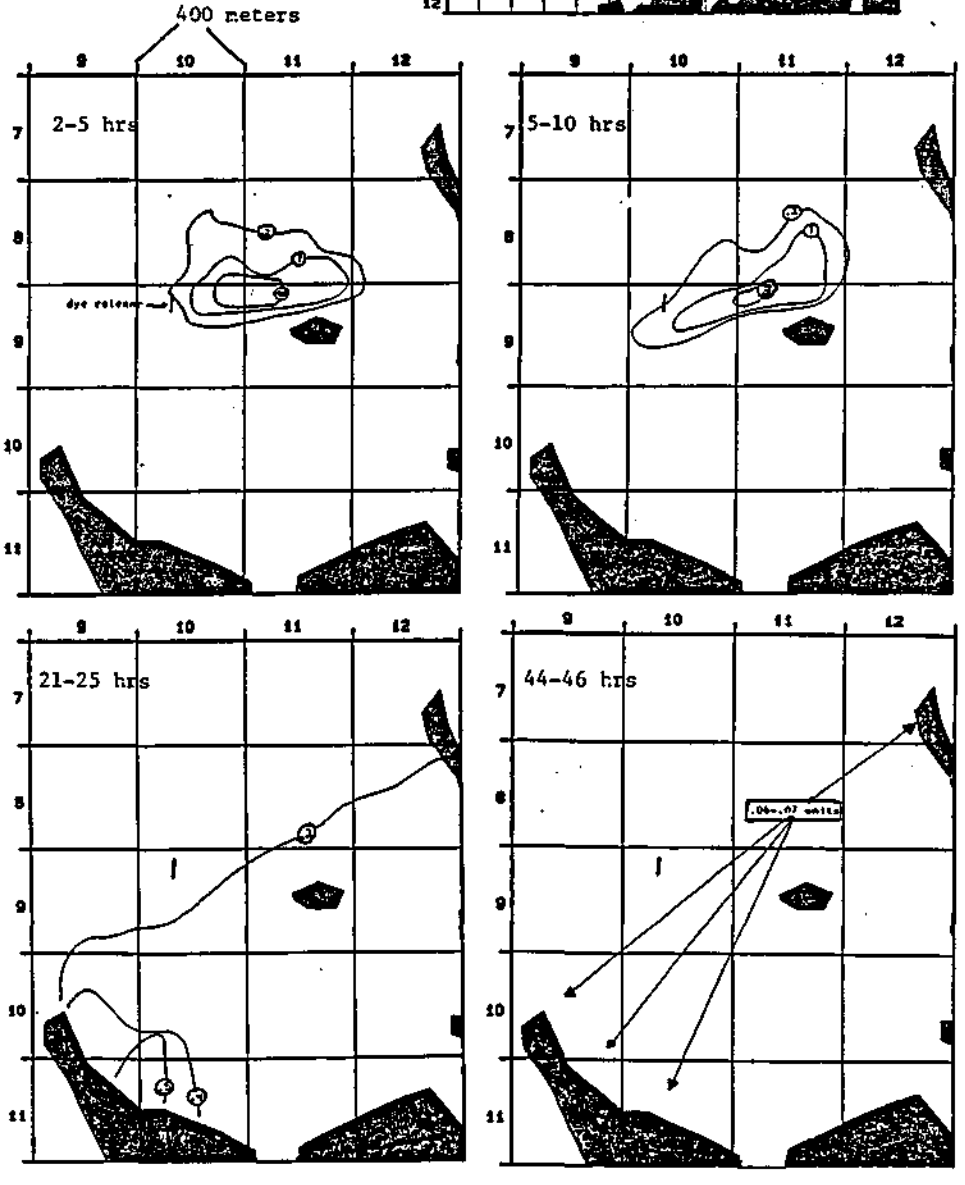

Figure 23

Observed and Predicted Dye Movements
September 15-17, 1986

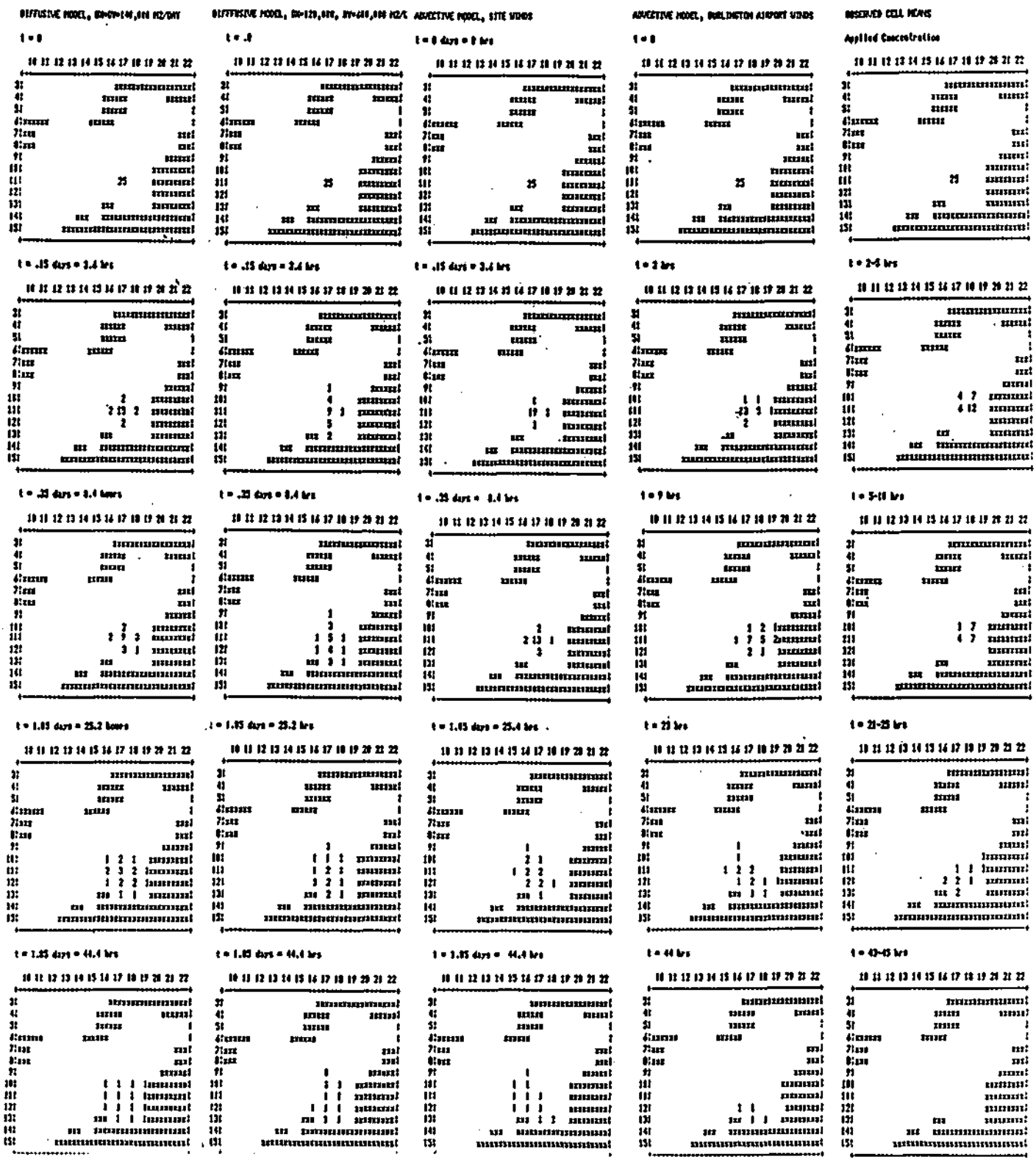

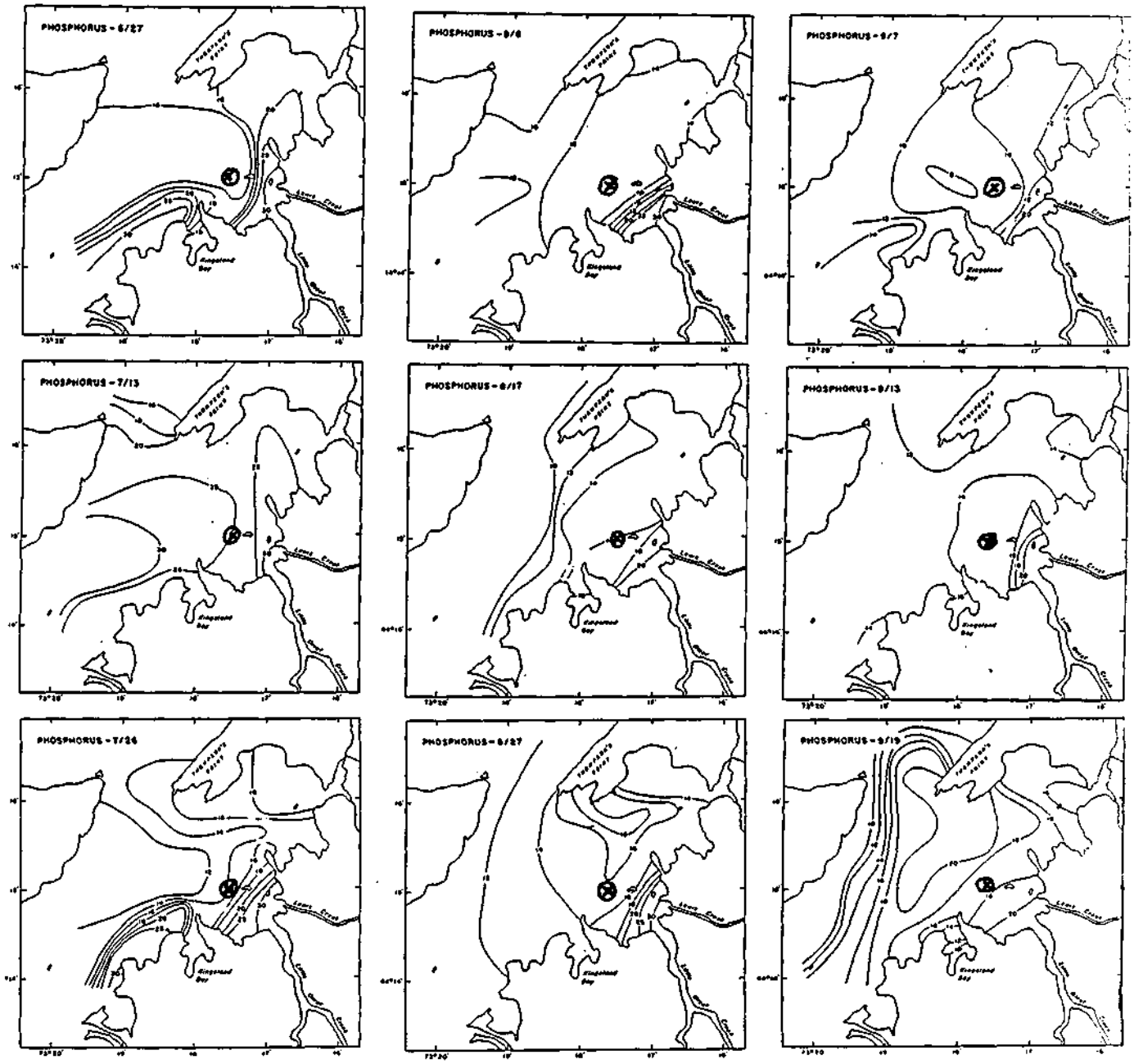

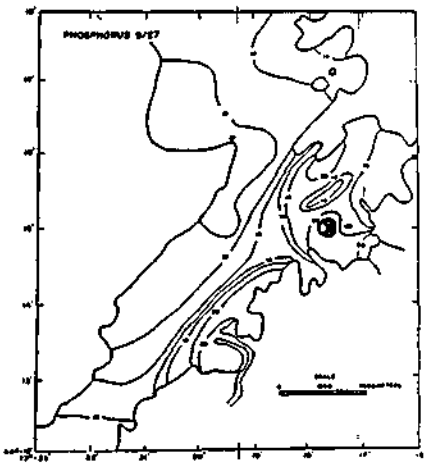

Figure 24
Phosphorus Contours in Study Region

June-September 1984
(Smeltzer,1985)

Figure 25
Wind Load vs. Direction

Burlington Airport
August-September 1984

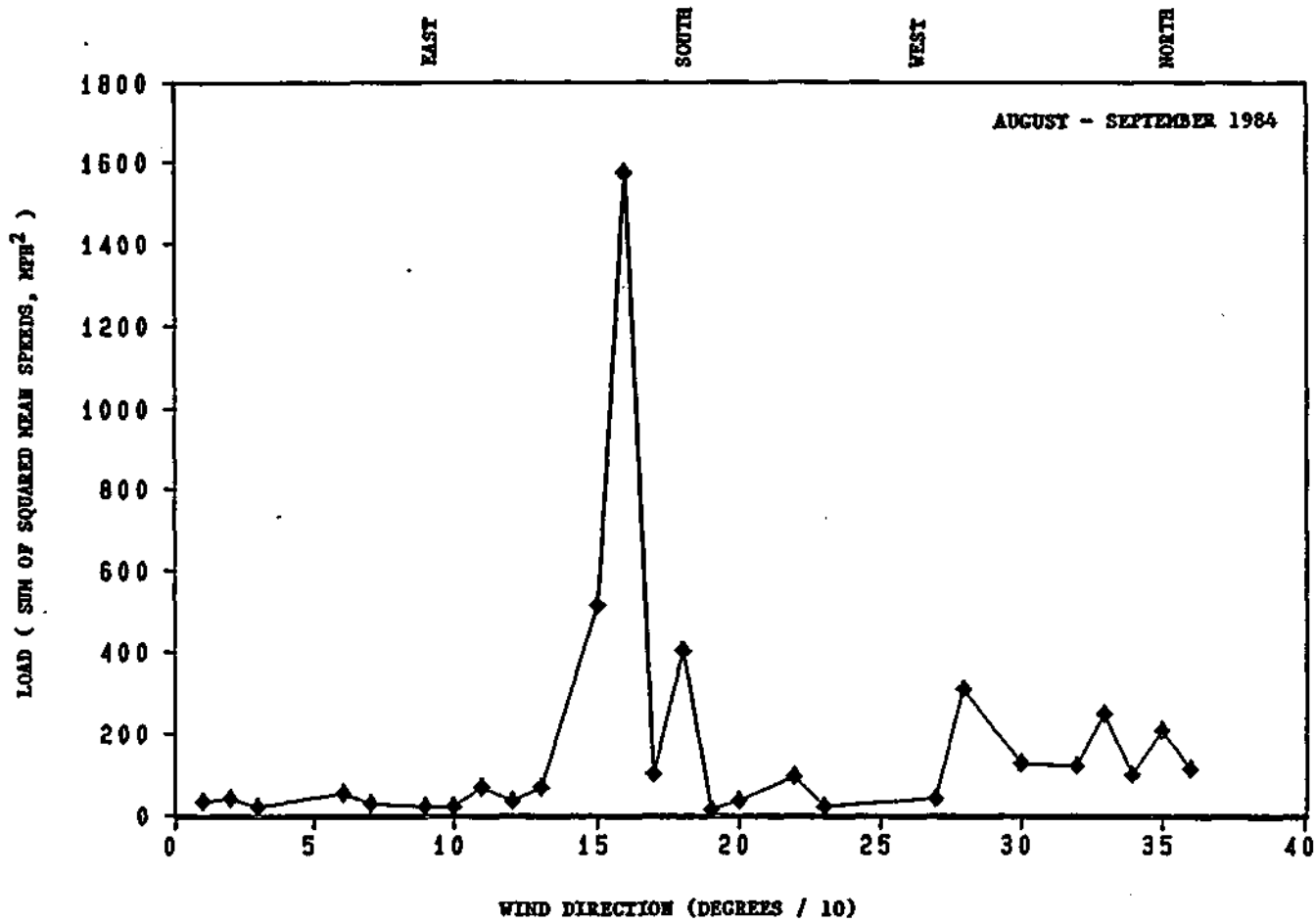

Figure 26
Balanced Flow Velocities

Southeast Wind
Mean Speed = 8.7 mph
Velocities in centimeters/sec x 10

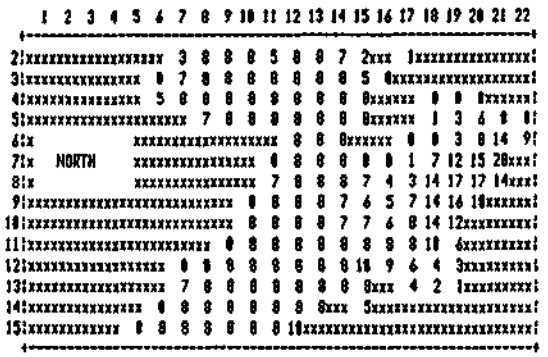

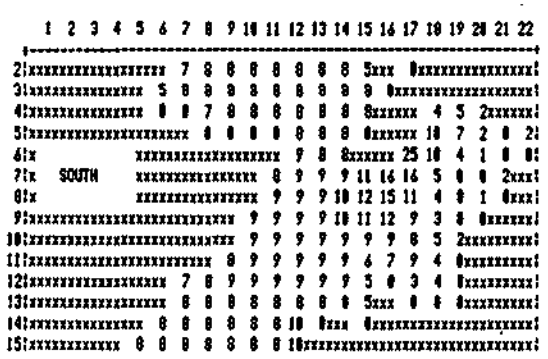

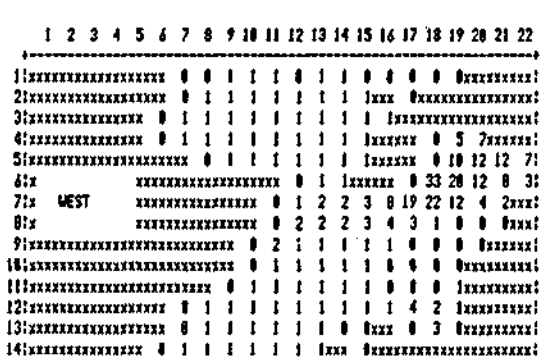

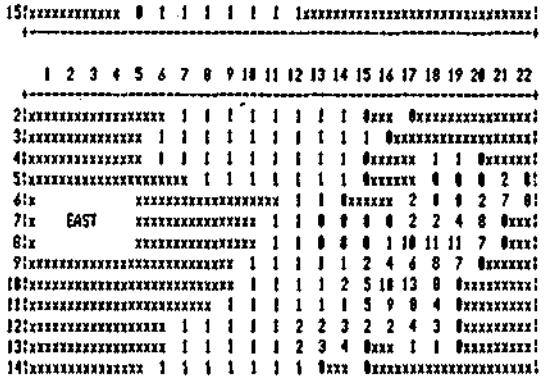

Figure 27
Dispersion Coefficient Calibration

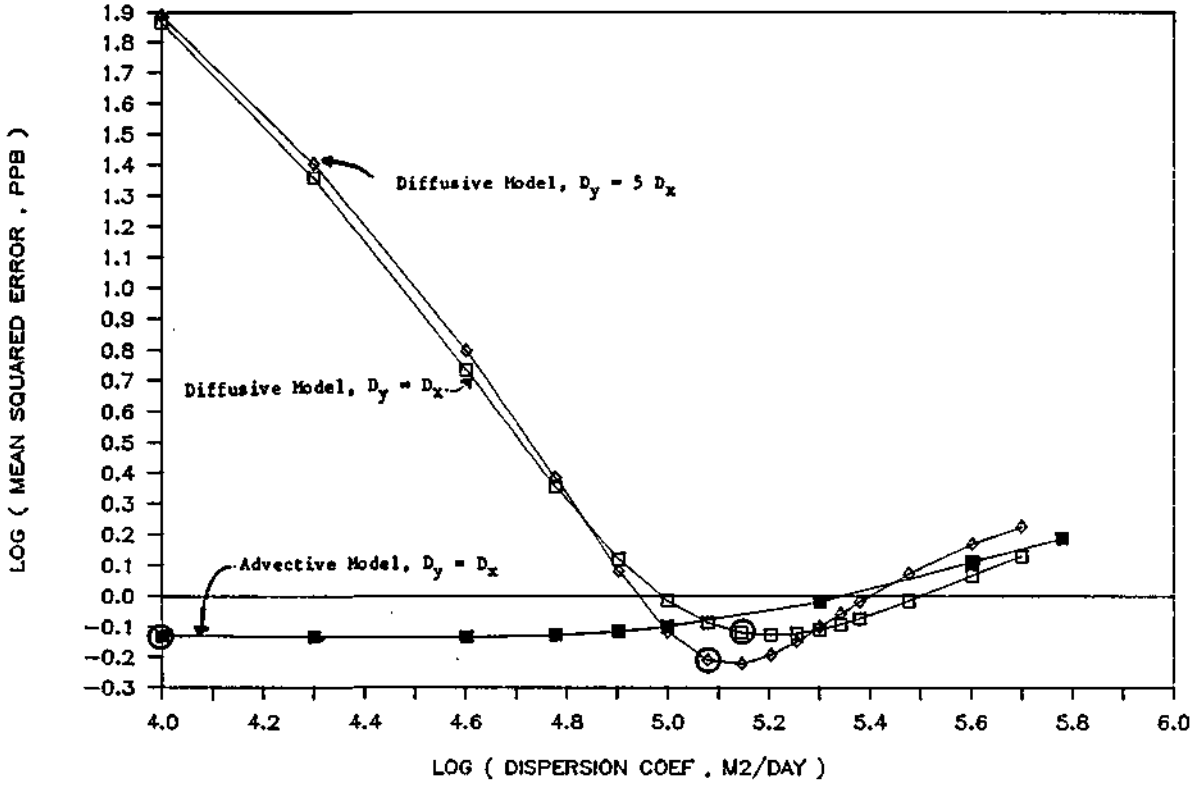

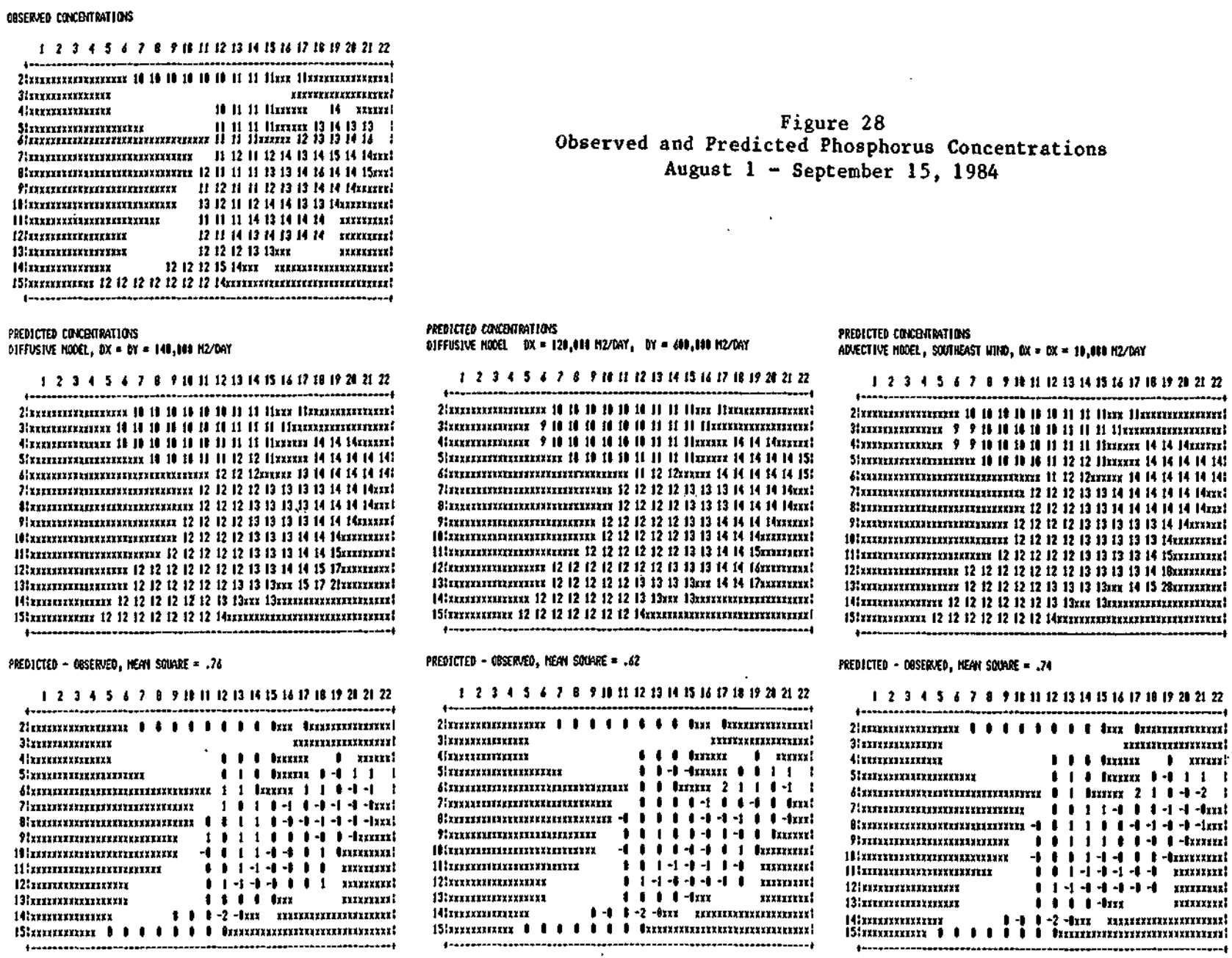

Figure 28
Observed and Predicted Phosphorus Concentrations
August 1 - September 15, 1984

Figure 29

Observed and Predicted Dye Concentrations
Steady Dye Release - August-September 1984

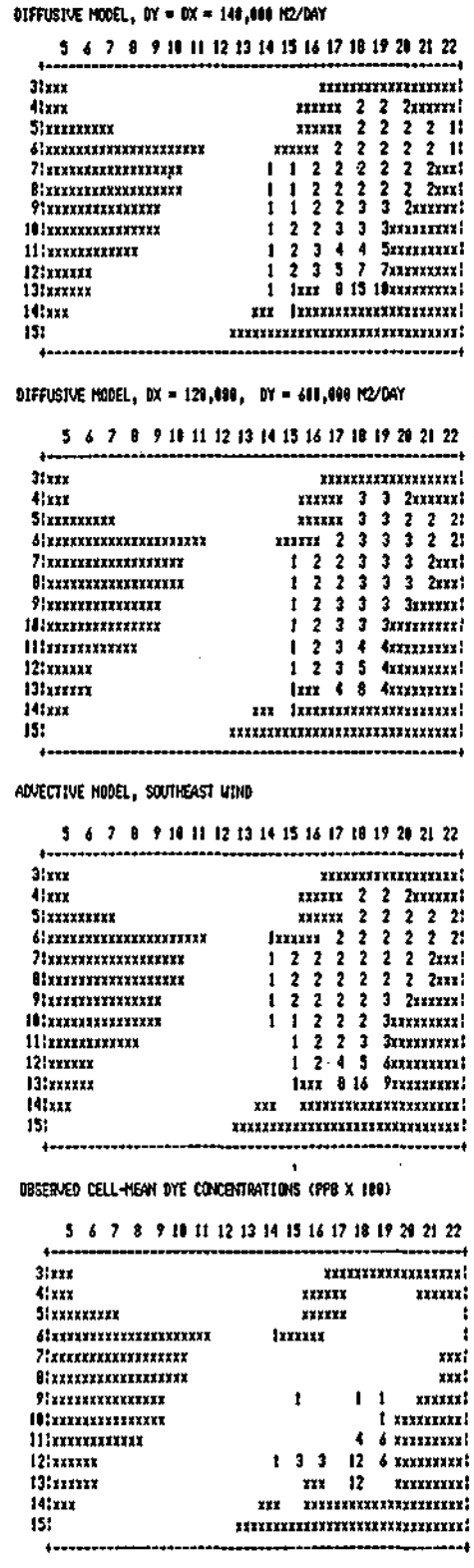

Figure 30

Predicted Hatchery Impacts
August Loading Conditions

Increases in Cell Phosphorus Concentrations (ppb x 10)

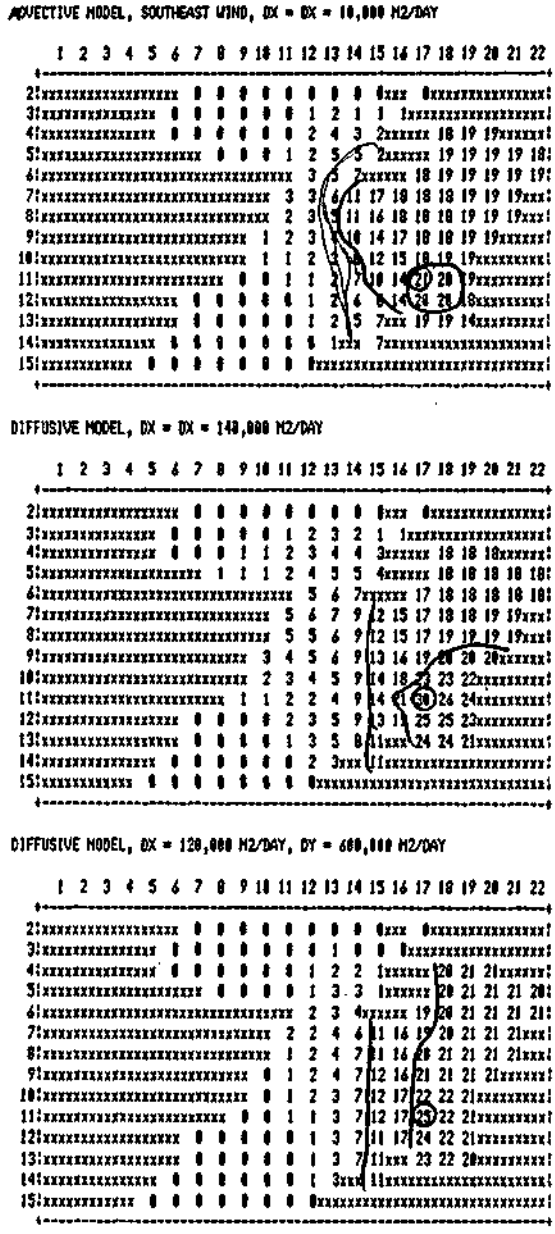

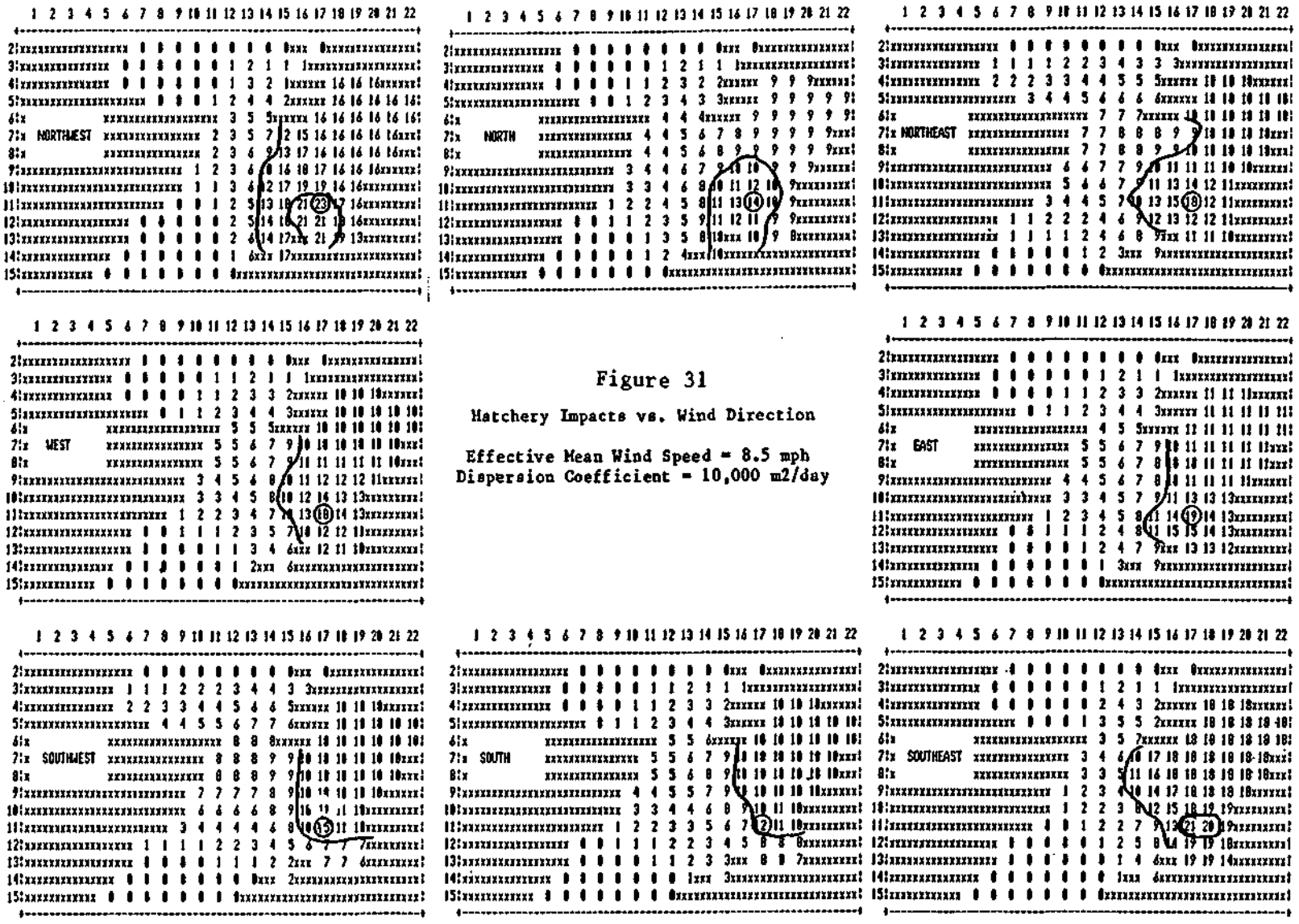

Figure 31

Hatchery Impacts vs. Wind Direction

Effective Mean Wind Speed = 8.5 mph
Dispersion Coefficient = 10,000 m2/day

Increases in Cell Phosphorus Concentrations (ppb x 10)

Figure 32

Simulation of Hatchery Impact under 1984 Wind Loads

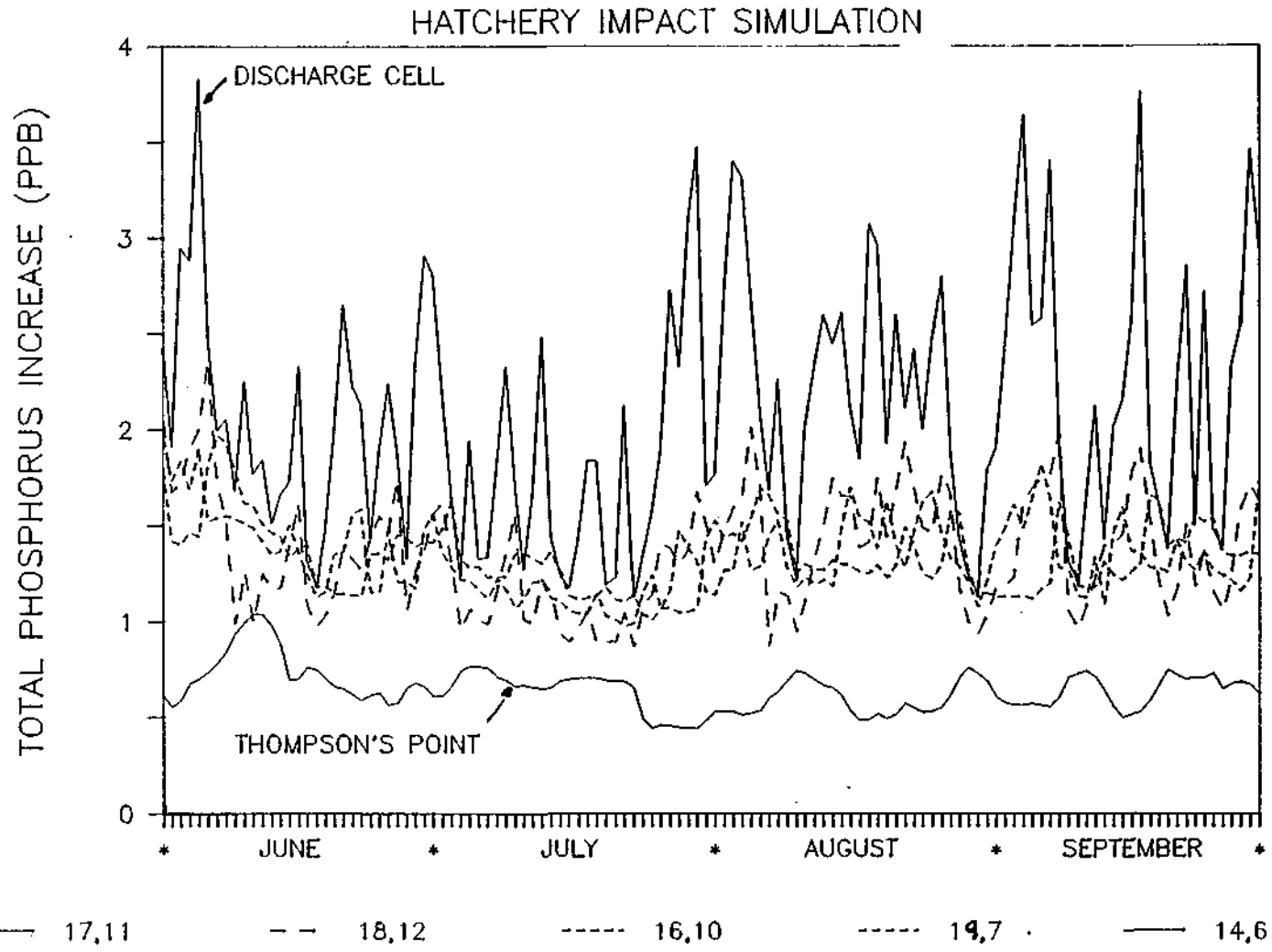

Column, Row of Simulation Grid (see Figure 1 for Locations)